energies

MDPI

Review

Energy and Thermal Performance Analysis of PCM-Incorporated Glazing Units Combined with Passive and Active Techniques: A Review Study

Hossein Arasteh [1], Wahid Maref [1,*] and Hamed H. Saber [2]

[1] Department of Construction Engineering, École de Technologie Supérieure (ÉTS), University of Québec, Montréal, QC H3C 1K3, Canada
[2] Prince Saud bin Thuniyan Research Center and Mechanical Engineering Department at Jubail Industrial College, Royal Commission of Jubail and Yanbu, Jubail 31961, Saudi Arabia
* Correspondence: wahid.maref@etsmtl.ca

Abstract: The building envelope provides thermal comfort, an excellent visual view, and sunlight for the occupants. It consists of two parts: (i) an opaque (non-transparent) part (e.g., walls and roofs) and (ii) a transparent part (e.g., windows, curtain walls, and skylight devices). Recently, the use of fully-glazed facades, especially in large cities, has increased due to their aesthetical and structural advantages. This has led this study to review the performance of the currently passive smart glazing technologies. Phase Change Materials (PCMs) as latent energy storage material is the focus of this review, as well as other individual and combined techniques, including shading systems, solar cells (photovoltaic), and chromogenic (thermotropic and thermochromic) materials. PCM-integrated glazing systems have been extensively studied and rapidly developed over the past several decades from the standpoint of unique system designs, such as passive, active, and passive/active mixed designs, intelligent management, and sophisticated controls. In the academic literature, numerous studies on PCM-integrated building envelopes have been conducted, but a comprehensive review of PCM-integrated GUs combined with other passive and active techniques using dialectical analysis and comparing the climatic conditions of each study using Köppen-Geiger climate classification climate classification has been performed only rarely. Consequently, the primary objective of this study is to reduce this discrepancy for all types of glazing, excluding glazed roofs. This review article also contains literature tables as well as highlights, limitations, and further research suggestions at the end of each subsection.

Keywords: smart glazing; PCM; solar photovoltaic; thermotropic; thermochromic; Köppen-Geiger climate classification

Citation: Arasteh, H.; Maref, W.; Saber, H.H. Energy and Thermal Performance Analysis of PCM-Incorporated Glazing Units Combined with Passive and Active Techniques: A Review Study. *Energies* **2023**, *16*, 1058. https://doi.org/10.3390/en16031058

Academic Editor: Przemysław Brzyski

Received: 16 December 2022
Revised: 16 January 2023
Accepted: 17 January 2023
Published: 18 January 2023

1. Introduction

Residential and building construction together account for about one-third of global final energy consumption and almost 15% of direct CO_2 emissions (40–48% direct and indirect CO_2 emissions), according to the International Energy Agency (IEA), as shown in Figure 1 [1]. Buildings and building construction continue to require more energy as a result of increased energy availability in emerging nations, rising air conditioning demand in tropical regions, increased ownership and usage of energy-intensive equipment, and quick development in building floor space. Energy trends in the building sector prove the high participation of buildings' heating and cooling share in energy use and CO_2 emissions. If this trend continues, more than 50% of the total energy consumed in the buildings will be used for space cooling and heating up to 2050 [1]. Therefore, applying scientific methods to decrease energy consumption and, consequently, CO_2 emissions in this sector could save the environment and reduce the consequences of global warming to a great extent.

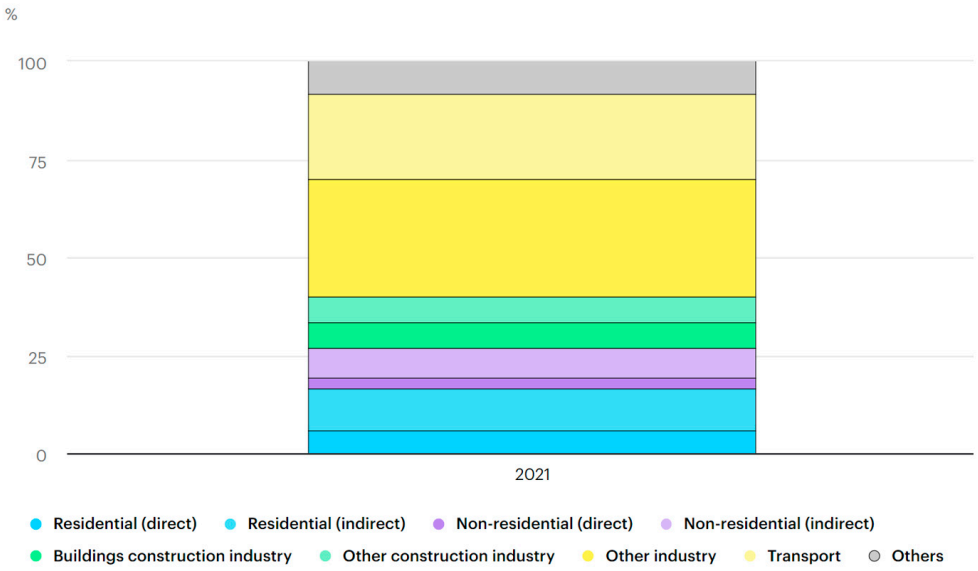

Figure 1. Global energy and process emissions from buildings, including embodied emissions from new construction, 2021 [1].

The building envelope provides a comfortable zone for the indoor space, including thermal and moisture comfort, acting as a shield against the largely variable and mostly undesired outdoor conditions. In recent years, numerous researchers have adopted various passive and active techniques to enhance the energy performance of the building envelope. Passive options include natural ventilation, solar radiation, and nighttime radiation from the earth and sky, whereas active solutions include mechanical ventilation and active cooling/heating of water or fluids. Active ventilation and active water-based cooling systems, which improve the system's controllability, heat dissipation, and cooling, consequently boosting the system's performance, are advantages of active systems over passive techniques. The disadvantages include the energy consumption of pumps and fans, the possibility of liquid leakage, and the high cost of maintenance, etc. [2]. Utilizing Phase Change Materials (PCMs) as a passive approach incorporated into the building envelope has lately garnered the interest of researchers due to the high latent energy storage resulting in a greater thermal mass for structures. PCMs have been incorporated into the building envelope's transparent part, which includes windows [3], curtain walls [4], and glazed roofs [5], and the opaque part that includes walls [6], ceilings [7], and floors [8]. The usage of PCMs can play a crucial role in managing the indoor temperature, transferring the peak load to off-peak hours, and reducing the energy required for space cooling and heating; nevertheless, further scientific research is required based on recent review studies on PCMs [9–12].

Glazing components, such as windows, glazing facades, and glazed roofs, allow daylighting, views of the outdoors, and passive solar gain. Overall, 30% of the building's energy consumption is accounted for by the glazed portions of the building envelope, and when there is a large window-to-wall ratio (WWR), this can grow to 60% by using windows and 90% by using curtain walls [13]. Concerning the thermal effect of WWR on building energy efficiency, Saber and Hajiah [14] developed a numerical model to examine the energy performance of PCM-incorporated building envelopes (walls and roofs) in different WWRs ranging from 10 to 70 percent. They discovered that WWRs of 10% and 40% produce the lowest and largest total annual loads, respectively. Despite the fact that several studies have been conducted on energy-saving methods for the glazing unit (GU) parts of a building, this part still suffers from a high solar transmittance factor, high thermal conductivity (low thermal resistance), and low thermal mass [15].

The type of structure and the climate of the building's location are two of the most powerful aspects determining the energy-saving technologies of glazing units. Based on

the Köppen-Geiger climate classification, there are five major climate types, including (A) tropical, (B) arid, (C) temperate, (D) cold, and (E) polar, and the sub-divisions of these five climatic types (see Table 1) [16]. In addition, Figure 2 depicts the world Map of Köppen-Geiger climate classification updated with mean monthly CRU TS 2.1 temperature and VASClimO v1.1 precipitation data for the period 1951 to 2000 on a regular 0.5 degree latitude/longitude grid. In what follows, all the reviewed studies are designated to a Köppen-Geiger climate class type [16]. Figure 2 corresponds a code to each location with a specific climatic condition. Hence, locations with similar Köppen-Geiger codes to each other can be treated almost the same.

Table 1. Köppen-Geiger climate classification descriptions and corresponding criteria [16].

1st	2nd	3rd		Description	Criterion [a]
A				**Tropical**	Not (B) & $T_{cold} \geq 18$
	f		-	Rainforest	$P_{dry} \geq 60$
	m		-	Monsoon	Not (Af) & $P_{dry} \geq 100 - MAP/25$
	w		-	Savannah	Not (Af) & $P_{dry} < 100 - MAP/25$
B				**Arid**	$MAP < 10 \times P_{threshold}$
	w		-	Desert	$MAP < 5 \times P_{threshold}$
	s		-	Steppe	$MAP \geq 5 \times P_{threshold}$
		h	-	Hot	$MAT \geq 18$
		k	-	Cold	$MAT < 18$
C				**Temperate**	Not (B) & $T_{hot} \geq 10$ & $0 < T_{cold} < 18$
	s		-	Dry summer	$P_{sdry} < 40$ & $P_{sdry} < P_{wwet}/3$
	w		-	Dry winter	$P_{wdry} < P_{swet}/10$
	f		-	Without dry season	Not (Cs) or (Cw)
		a	-	Hot summer	$T_{hot} \geq 22$
		b	-	Warm summer	Not (a) & $T_{mon10} \geq 4$
		c	-	Cold summer	Not (a or b) & $1 < T_{mon10} < 4$
D				**Cold**	Not (B) & $T_{hot} > 10$& $T_{cold} \leq 0$
	s		-	Dry summer	$P_{sdry} < 40$& $P_{sdry} < P_{wwet}/3$
	w		-	Dry winter	$P_{wdry} < P_{swet}/10$
	f		-	Without dry season	Not (Ds) or (Dw)
		a	-	Hot summer	
		b	-	Warm summer	Not (a) & $T_{mon10} \geq 4$
		c	-	Cold summer	Not (a, b, or d)
		d	-	Very cold winter	Not (a or b) & $T_{cold} < -38$

Table 1. *Cont.*

1st	2nd	3rd	Description	Criterion [a]
E			**Polar**	Not (B) & $T_{hot} \leq 10$
	T	-	Tundra	$T_{hot} > 0$
	F	-	Frost	$T_{hot} \leq 0$

[a] Variable definitions: MAT = mean annual air temperature (°C); T_{cold} = the air temperature of the coldest month (°C); T_{hot} = the air temperature of the warmest month (°C); T_{mon10} = the number of months with air temperature >10 °C (unitless); MAP = mean annual precipitation (mm y^{-1}); P_{dry} = precipitation in the driest month (mm $month^{-1}$); P_{sdry} = precipitation in the driest month in summer (mm $month^{-1}$); P_{wdry} = precipitation in the driest month in winter (mm $month^{-1}$); P_{swet} = precipitation in the wettest month in summer (mm $month^{-1}$); P_{wwet} = precipitation in the wettest month in winter (mm $month^{-1}$); $P_{threshold}$ = 2 × MAT if >70% of precipitation falls in winter, $P_{threshold}$ = 2 × MAT + 28 if >70% of precipitation falls in summer, otherwise, $P_{threshold}$ = 2 × MAT + 14. Summer (winter) is the six-month period that is warmer (colder) between April–September and October–March.

The construction industry has shifted toward the usage of lightweight structures due to its major benefits, such as less material consumption and shorter construction times. Using curtain walls as building glazing facades rather than conventional windows or masonry as a lightweight building technology [17] has resulted in the creation of nearly fully-glazed buildings and skyscrapers, particularly in large cities. It also provides an architecturally desirable view for the residents and a picturesque view of the front from the interior. In contrast, the low thermal resistance of glazing units and their increased use in recent years have piqued the interest of researchers seeking to maximize the energy performance of glazing units by taking into account the smallest change in optical qualities. Yu et al. [18] addressed to the paradoxical influence of daylight on indoor thermal and visual comfort and energy use, stating that a "thermal-daylighting balance" must be struck between them. The authors determined that the thermal daylighting balance is dependent on the individual properties of the building envelope and the local climate.

PCM-integrated glazing systems have been extensively investigated and rapidly developed over the past several decades from the perspectives of unique system designs, including passive, active, and passive/active combined designs, intelligent management, and sophisticated controls. In the academic literature, numerous studies have been conducted on PCM-integrated building envelopes, but a comprehensive review of PCM-integrated GUs combined with other passive and active techniques using dialectical analysis and comparing the climatic conditions of each study using Köppen-Geiger climate classification climate classification has been conducted only rarely. Therefore, the primary purpose of this study is to bridge this gap for all types of glazing, except glazed roofs.

This review is organized into two main sections: glazing unit technologies with and without PCM use. The first section is a comprehensive review of PCM-incorporated GUs only and combined with passive and active technologies comprising the vast majority of related studies. This section is divided into three subsections: PCM-incorporated multi-layered GUs, PCM-incorporated shading systems of GUs, and PCM/PV-incorporated multi-layered GUs. In the absence of PCMs, the second section reviews the GU technologies alone and in conjunction with passive and active technologies. This section does not include the large bulk of relevant articles, as there are countless in the literature and only some are chosen. It is subdivided into three subsections, including photovoltaic (PV) windows, shading systems (without PCM), and thermotropic and thermochromic materials in GUs. At the end of each section there are challenges and opportunities, as well as Köppen-Geiger climate classification influences on smart glazing systems.

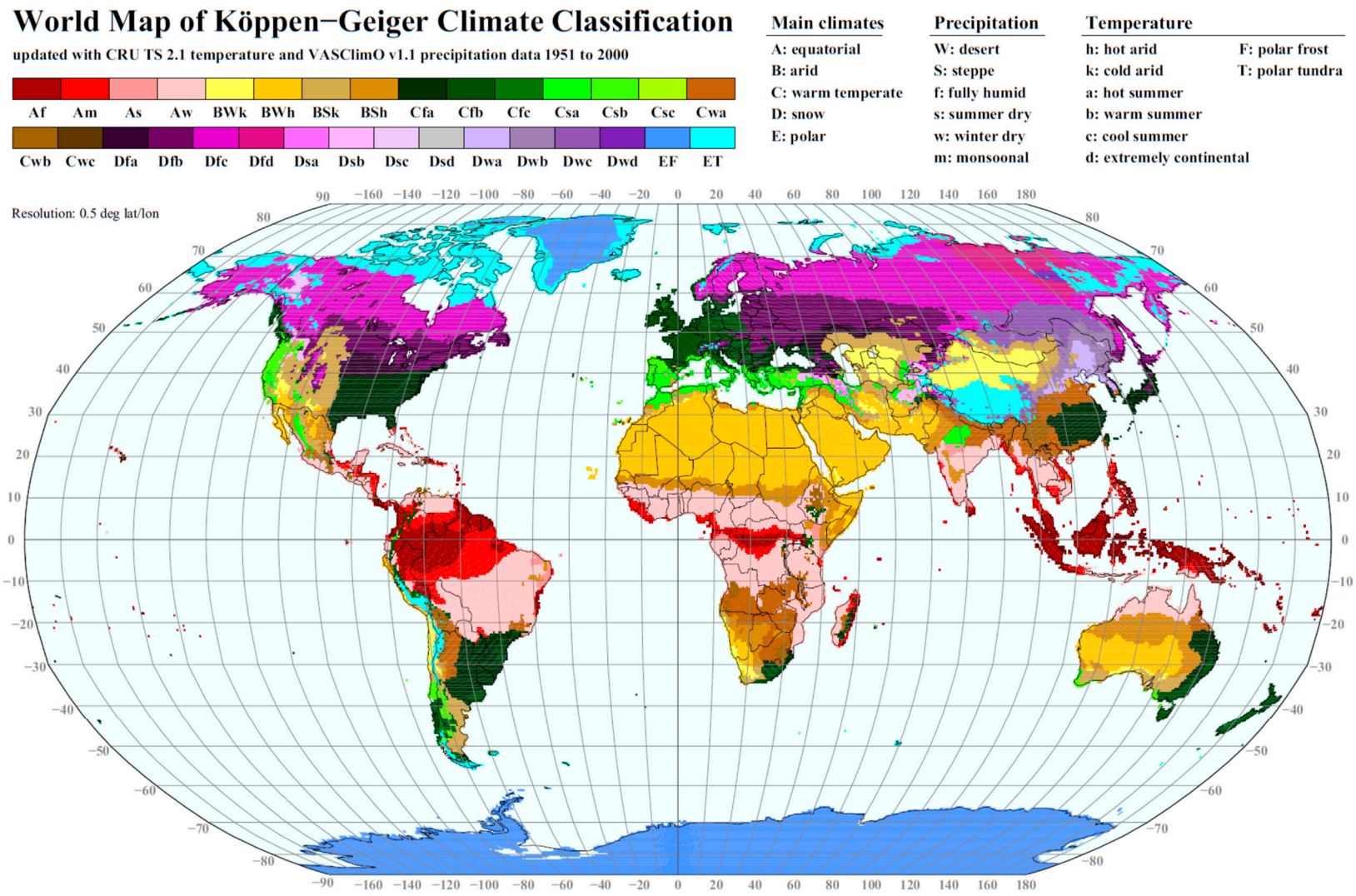

Figure 2. World Map of Köppen-Geiger climate classification updated with mean monthly CRU TS 2.1 temperature and VASClimO v1.1 precipitation data for the period 1951 to 2000 on a regular 0.5 degree latitude/longitude grid [19].

The papers acquired using the keyword "PCM glazing window" were downloaded, classified, and incorporated into section one of this article. By navigating through so many Google Scholar pages until articles were unrelated to the chosen keyword, nearly all relevant papers were downloaded. Some selected articles were downloaded with the subsection titles of section two for the individual application of the technology without PCM for the technologies employed as a combined approach with PCM. Figure 3 depicts the number of reviewed papers in each subsection of Sections 1 and 2.

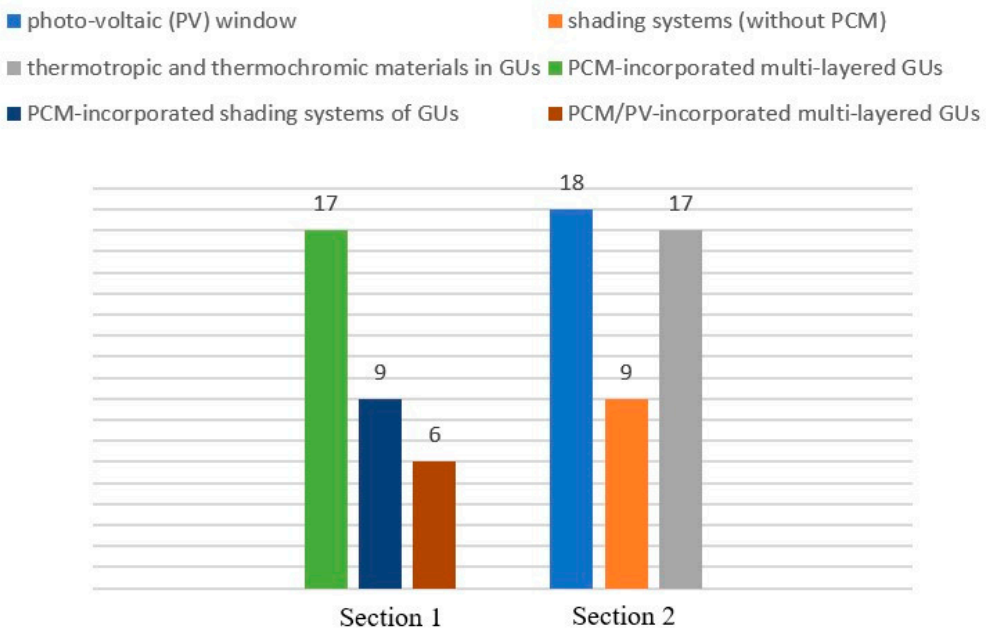

Figure 3. The number of reviewed papers in each subsection of Sections 1 and 2.

2. Phase Change Materials

Thermal energy storage (TES) is a viable method for improving the energy efficiency of buildings and other applications, including concentrated solar power plants [20], PV panels [21], and heat pump systems [22]. TES systems are classified into two main categories as (i) thermal and (ii) thermochemical energy storage. Due to unclear cost and longevity, the second use has not shown to be beneficial [23]. The first has already been used in many applications and is classified as sensible and latent heat storage [24]. Table 2 compares the thermal storage properties of sensible and latent heat. This table demonstrates that the energy storage capacity of a latent heat system is 5 to 13 times that of a sensible heat system [25], demonstrating the significant potential of such materials to improve the thermal mass of buildings.

Table 2. Comparing the sensible and latent heat of TES materials for 15 K temperature increase and 300 kWh energy storage [25].

Material Property	**TES Sensible Heat**		**TES Latent Heat**	
Material	Rock	Water	Organic PCM	Inorganic PCM
Density (kg/m^3)	2240	1000	800	1600
Specific heat (kJ/(kg·K))	1	4.2	2	2
Latent heat (kJ/kg)	-	-	190	230
Latent heat (kJ/m^3)	-	-	152	368
Mass of storage for 10^6 J (kg)	67,000	16,000	5300	4350
Volume of storage for 10^6 J (m^3)	30	16	6.6	2.7
Mass of relative storage (-)	15	4	1.25	1
Volume of relative storage (-)	11	6	2.5	1

The driving force for the process of charging and discharging the storage determines whether a system is passive or active; active systems use a pump or fan for the process, whereas in passive systems, the phase change is caused by a temperature difference between the environment and the storage [23]. PCMs supply considerable latent heat throughout their phase transition at a constant temperature, which is a desirable property, particularly during the phase change from solid to liquid and vice versa, as shown in Figure 4 [26]. The phase change could occur in the solid, liquid, and gas states through vaporization and condensation and in solid and liquid through freezing and melting. In building envelopes, solid–liquid and solid–solid phase changes are the most common [27]. Figure 4 illustrates the fluctuating temperature of PCM's storing heat. As depicted in the figure, when the temperature of the PCM exceeds its melting temperature (MT), the chemical bonds of its molecules begin to dissolve in an endothermic process, allowing the PCM to absorb heat and shift from a solid to a liquid phase. In contrast, as the temperature drops and hits the PCM's freezing point, the molecules' chemical bonds begin to renew in an exothermic process, culminating in the PCM's transition from a liquid to a solid state, a process known as discharge [28].

Solid–liquid PCMs are divided into three major categories: organic, inorganic, and eutectic, as well as the subgroups depicted in Figure 5 [26]. Each class has distinct thermal qualities that can be employed depending on the storage system's operational conditions. Figure 6 [26] depicts the melting range and enthalpy of the specified PCM classes. The MT range of paraffin as an organic form of PCM is within a suitable range for heating and cooling applications in buildings, as depicted in this figure. This material (paraffin) has been utilized in the majority of GU-related applications due to its wide range of phase transition temperatures within a thermal comfort range, low cost, and good optical and light transmission properties [29].

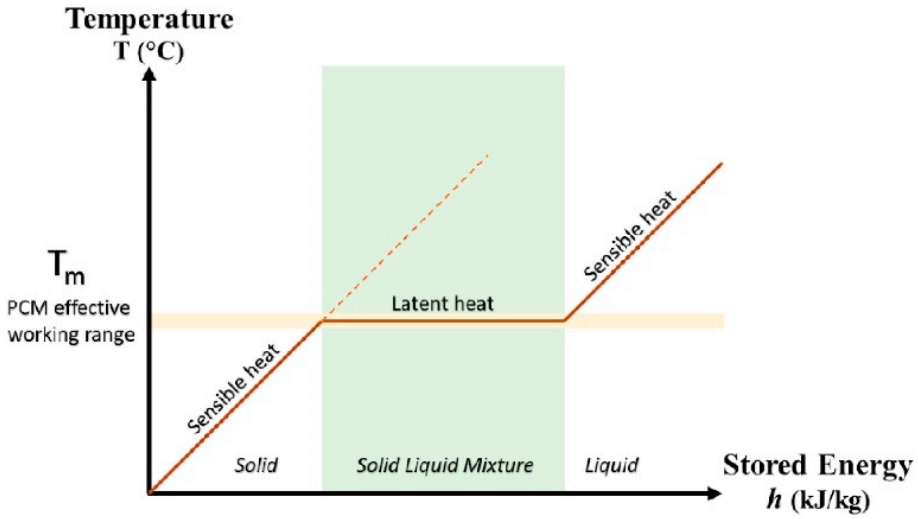

Figure 4. PCM energy storage by temperature variations [26].

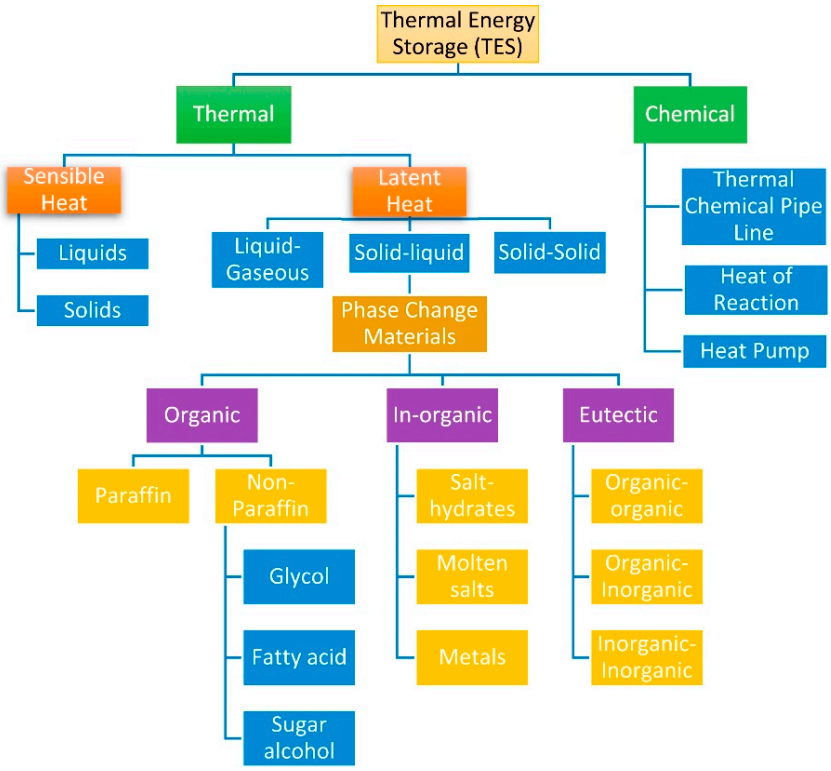

Figure 5. Classification of PCMs [26].

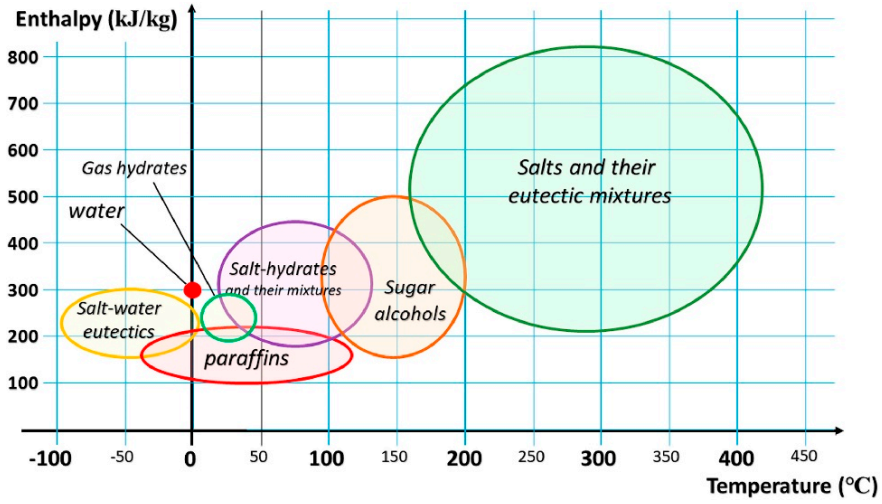

Figure 6. Temperature and enthalpy ranges for various PCMs [26].

3. Energy-Saving Technologies of GUs

Different energy-saving technologies, applied to the transparent parts of building envelope, have been studied by the researchers, including multiple-glazing windows, blind and shading devices, exhaust air windows, water glazing systems, thermotropic and thermochromic materials, low-e coatings, aerogels, PV systems, Prisma solar glasses, different insulating methods, different laminated glasses, phase change materials, and so forth [30]. The following is a summary and discussion of the aforementioned technologies, with an emphasis on the application of PCMs in GUs. Since the primary purpose of this study is to examine the possible energy-saving technologies coupled with PCMs applied to curtain walls, all glazing units, excluding glazed roofs, were examined. In addition, the examined research is divided into two categories: (i) technologies of GUs with PCM and (ii) technologies of GUs without PCM.

3.1. Technologies of GUs with PCM Utilization

3.1.1. PCM-Incorporated Multi-Layered GUs

In numerous studies, PCMs have been employed in double-glazed units (DGUs) to improve the thermal performance of the system while maintaining the optical and light transmittance that resident's desire. Goia et al. [31] conducted a numerical and experimental investigation to compare the thermal performance of PCM-incorporated double glazing windows (DGWs) to that of standard DG windows in warmer areas (Cfa). Figure 7 depicts the test cells employed by the authors, one DGU with PCM and the other without PCM. For their research, the authors utilized RT35 paraffin with a nominal MT of 35 °C. The results demonstrated that the PCM-DG system has the potential to improve the indoor thermal environment, and its efficacy increases as solar irradiation rises. On a cloudy day, however, the thermal comfort produced by the two systems is the same. The presence of PCM in the fenestration system minimizes glare risk and improves eye comfort, according to the study. Later, Goia et al. [32] experimentally evaluated the energy performance of a PCM-DG system in a similar study, using the same test cells as in [31]. They utilized the identical weather and PCM data as in [31]. Comparing the PCM-DG window to the conventional DG window, they determined that the PCM-DG window results in a 50% decrease in summertime energy gain. However, they argued that in the winter, the energy performance is more complex and requires additional study, as the daytime heat loss lowers while the direct solar gain decreases dramatically. In addition, they suggested control measures such as night ventilation to improve the system's performance. King et al. [33] conducted an experiment to determine the thermal performance of a PCM-DG window in Coimbatore, India (Aw) during the cooling season. As PCM material, the paraffin RT35 with MT of 29–36 was chosen. The PCM-DG window reduces energy usage by 3.76%, temperature fluctuations from 21 °C to 11 °C, interior air temperature by 9 °C, and inner glass temperature by 8.5 °C, according to the findings of the study's authors. Liu et al. [34] executed an additional experiment to examine the thermal and optical performance of PCM-DG windows with varying solar energy intensities including 270 (W/m^2), 600 (W/m^2), and 950 (W/m^2). The authors utilized three MTs of 18 °C, 26 °C, and 32 °C with paraffin wax PCM. Figure 8 depicts the solid and liquid states of the PCM used by the authors and the transmittance of the studied PCMs with different MTs. This figure shows that the transmittance in liquid phase is almost 1 regardless of the MT of PCM, while the PCM's MT significantly affects the transmittance in solid phase. Considering PCM's volume growth during the phase change, these researchers filled 97% of the total volume between the panes with PCM. The results indicated that the glazing unit containing PCM in liquid form has a 50% transmittance. Moreover, in order to maintain the optical performance of the GU, these researchers recommend avoiding PCM layers thicker than 16 mm. Tafakkori and Fattahi [35] in Tehran, Iran (Bwh), proposed and evaluated various configurations for PCM-DG windows of simple cubic (as the reference case), partition-arranged simple cubic, simple cubic with a cylindrical wall, trapezoidal prism, partition-arranged trapezoidal prism, and trapezoidal prism with the cylindrical wall to reduce energy losses from building envelope. These scientists utilized paraffin MG29 with a melting point of 27 °C. According to their findings, the proposed configurations reduce energy consumption by around 20%. Musial [36] numerically and experimentally analyzed the energy performance of a DG unit containing RT28 PCM with MT of 27.5 °C as a thermal accumulator unit inside the inner-pane space in Rzeszów, Poland (Cfb) instead of filling the cavity space between the panes of a DGU (see Figure 9). In the winter, the author demonstrated that the suggested system produces a 10% more desired daily heat balance than a DG unit with no PCM; however, in the summer, there was no significant change in the daily heat balance. During the cooling interval, the PCM storage unit was also discovered to be overheating. In another study, Musial and Licholai [37] implemented a PCM heat accumulator between the panes of a DG window with an external mobile shading system to examine its thermal performance through a numerical and experimental study during the summer season (June to August) in Rzeszów in Poland (Cfb), Naples

in Italy (Csa), and Tallinn in Estonia (Dfb). The author chose a eutectic combination of propyl palmitate and butyl stearate as the PCM. The results showed a 29.4% decrease in room overheating in summer for the system with PCM storage compared to the system without it. A reduction in the amount of heat flowing through the building was also reported as 5.5%, 29.4%, and 24.8% Tallinn, Rzeszów, and Naples, respectively. Durakovi et al. [38] also examined the use of PCM and water in a DG south-facing window as thermal storage materials in Sarajevo, Bosnia (Cfa) between June and December (25 °C in the summer and 4.5 °C in the winter) to evaluate their experimental performance. The paraffin RT27 was chosen as the PCM material. Compared to air-filled DG windows, the water glazing system exhibited a significantly more desirable damping temperature (more uniform and stable temperature values with fewer fluctuations) but a significantly less desirable average temperature. The PCM glazing system, on the other hand, has a promising average temperature and damping temperature.

Figure 7. Test cells composing DGU with clear glasses and DGU-PCM [31,32].

As depicted in Figure 10, Khetib et al. [39] explored the placement of PCM between the window frames of a DGW. They evaluated the impact of window angle variation from 0 (vertical mode) to 60° and space cavity depth on the PCM and window heat transfer. Between the window frames, n-eicosane was employed as the PCM with an MT of 37 degrees Celsius. Due to the decrease in natural convection heat transfer within the window, deviating a window from its vertical position by 60 degrees decreases heat transfer by 10%. It was also discovered that expanding the air gap to 40 mm decreases the Nusselt number by 44%. Moreover, it was demonstrated that the heat transmission decreases during the phase change of PCM from solid to liquid, but that PCM loses its heat transfer effectiveness when it totally melts. Gao et al. [40] researched the phase transition of the PCM in the solid state on the interior layer of the inner pane of a DGW, as demonstrated in Figure 11. Using EnergyPlus software, the optical and thermal performance of the solid–solid translucent PCM window was numerically studied. In warm, mixed, and cold regions, 3 mm PCM integration reduces building energy consumption by up to 9.4%, 6.7%, and 3.2%, respectively. Yang et al. [41] applied an optimization model to look into the optical characteristics of PCM-based nanofluid, namely the nanoparticle concentration and diameter in GUs. The PCM was paraffin wax and the nanofluid was TiO_2. The scientists concluded that increasing the nanoparticle diameter from 10 nm to 30 nm increases the scattering coefficient of PCM nanofluid by a factor of 28.7.

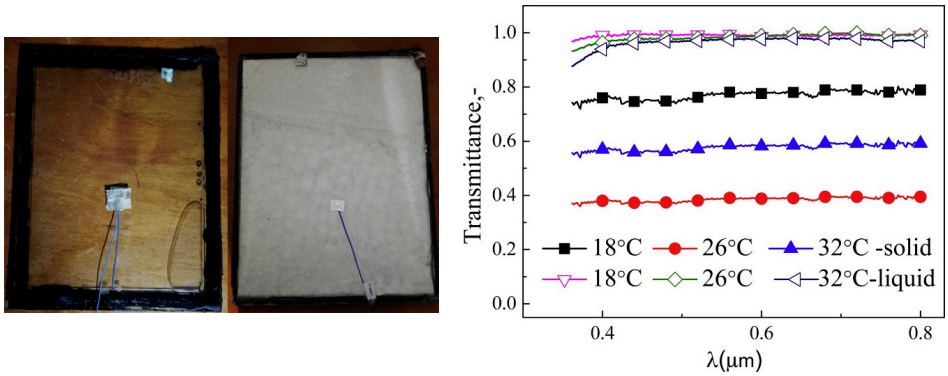

Figure 8. Paraffin wax PCM in liquid and solid phases along with their transmittance variations in different MTs [34].

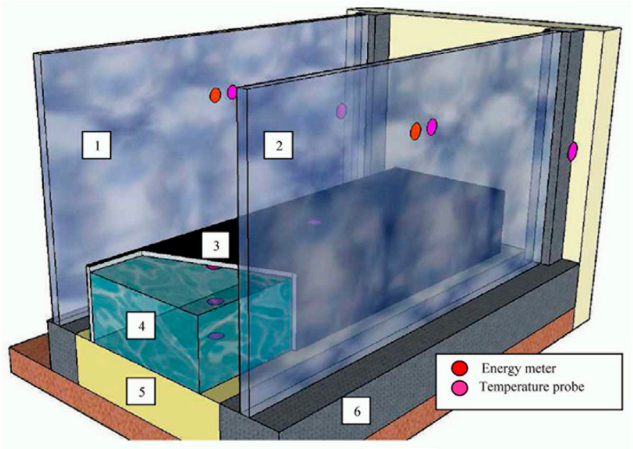

Figure 9. A schematic diagram of DGU containing PCM accumulator between the panes. 1—exterior glazing, 2—interior glazing, 3—thermal storage unit, 4—PCM, 5—XPS thermal insulation, 6—window frames [36].

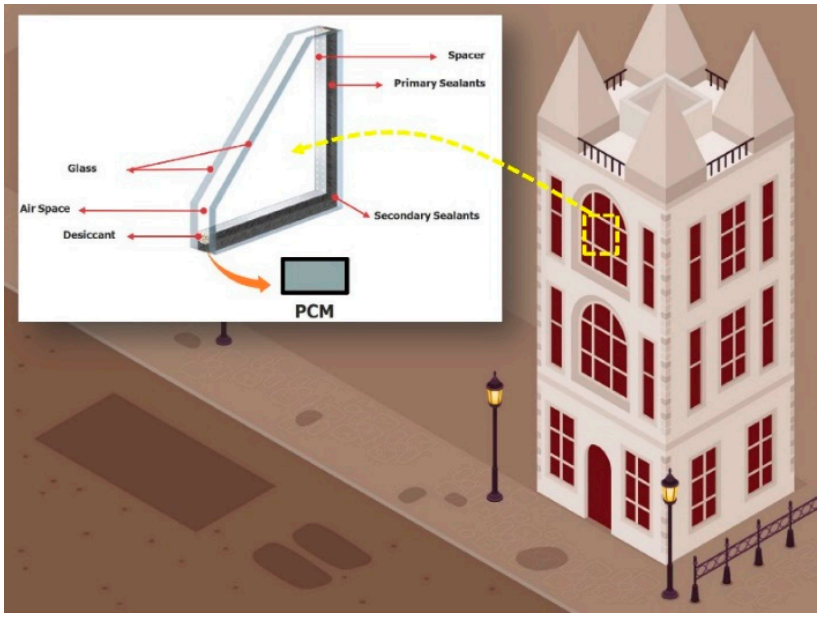

Figure 10. Schematic of fenestration system [39].

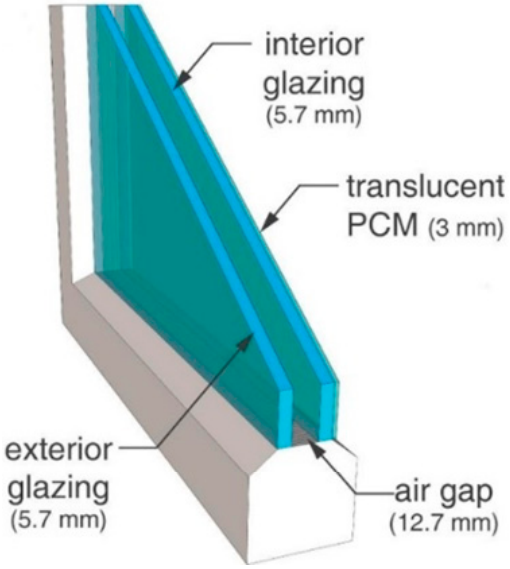

Figure 11. Schematic of DG system [40].

PCMs have also been used in triple-glazing (TG) and quadruple-glazing (QG) windows. In Nanjing, China (Cfa)., Li et al. [42] empirically and mathematically assessed the cooling and heating energy performance of a PCM-TG window. The numerical simulations were carried out utilizing ANSYS Fluent. The PCM material paraffin MG29 with an MT of 27–29 °C was inserted in the outside gap cavity space of the TG window, while the inner cavity was filled with air compared to a TGU and PCM-DGU with an entirely air-filled cavity. Using the PCM-TG window prevents overheating during the cooling time, as demonstrated by the findings. In a typical sunny summer day, comparing the PCM-TG window to the PCM-DG window and hollow TG window, 21.30% and 32.80% reductions in energy consumption were noted. Wieprzkowicz and Heim [43] evaluated the cooling and lighting energies, glare effect, and thermal and optical discomforts of a PCM-TG window in Lodz, Poland (Dfb), by means of a numerical and experimental investigation. Five PCMs of paraffin RT18HC, RT22HC, RT25HC, RT28HC, and RT31 were chosen to fill the outer cavity space of the glazing system, while Argon gas was used to fill the interior cavity space. The acquired results indicate that there is no optimal unit type of PCM for the system, and that employing PCMs with varied MTs is advantageous from an energy and optical standpoint, as liquid PCM provides an excellent view of the sky and visual comfort, although this is not true for solid PCM. The authors advised covering the lower half of the window with a PCM to ensure the occupant's optical view and filling the upper half of the window with a PCM to prevent overheating caused by energy demand. Considering applying PCM-QG windows, Liu et al. [44] tested the thermal performance of a south-facing four-glazed unit comprising PCM with MT of 25–28 °C between the two middle panes of the fenestration system numerically and experimentally during the winter time in Daqing, China (Dwa), which has a severe cold winter. The authors highlighted the significance of PCM thickness for the thermal efficiency of the glazed facade system. As a trade-off between improved thermal performance and reduced solar transmittance, it was also proposed that PCMs not exceed 20 mm in thickness. The purpose of Table 3 is to facilitate a clear comparison between the aforementioned research on the use of PCMs in GUs.

Table 3. Summary of PCM-incorporated multilayered GUs.

Ref.	PCM Type (MT °C)	Climate Code	Study Type	Envelope Element	Application	Findings and Remarks
[31]	RT35 paraffin (35)	Cfa	E, N	DGW	Cooling and heating	• On cloudy days, the performance of the two technologies (PCM-DGU and conventional DGU) is similar regarding thermal comfort, while the efficacy of PCM-DGU increases as solar irradiation rises. • The presence of a PCM in the facade can also positively influence visual comfort, as it may prevent glare.
[32]	RT35 paraffin (35)	Cfa	E	DGW	Cooling and heating	• The use of PCM in summer is promising while, its application in winter faces some challenges that need further research as the direct solar gain decreases dramatically. • They suggested control measures such as night ventilation to improve the system's performance.
[33]	RT35 paraffin (29–36)	Aw	E	DGW	Cooling	• The PCM-DG window reduces energy usage by 3.76%, temperature fluctuations from 21 °C to 11 °C, and interior air temperature by 9 °C.
[34]	Paraffin wax (18, 26, 32)	-	E	DGW	Cooling	• Considering PCM's volume growth during the phase change, the researchers filled 97% of the total volume between the panes with PCM. • The transmittance of the glazed unit is 50% when the PCM is liquid. • PCM thickness in glazed unit shouldn't exceed 16 mm for optical performance.
[35]	Paraffin, MG29 (27)	Bwh	N	DGW	Cooling	• Using PCM-DGU system causes 20% reduction in energy consumption and a decrease in the Nusselt number by a factor of 4.
[36]	RT28 paraffin (28)	Cfb	E, N	DGW	Cooling and heating	• Instead of filling the cavity between DGU panes, a PCM thermal accumulator is used. • Using PCM between the panes of the DGW caused 10% improvement in daily heat balance in heating seasons, while in cooling seasons, PCM accumulator had no significant impact on daily heat balance and experienced overheating.

Table 3. *Cont.*

Ref.	PCM Type (MT °C)	Climate Code	Study Type	Envelope Element	Application	Findings and Remarks
[37]	*n*–octadecane (25.05–26.11) *n*-eicosane (33.63–35.64) *n*-docosane (42.21–43.15)	Dwa	N	Exterior	Cooling and heating	• 44% reduction in cooling energy consumption and 34% improvement in thermal comfort are observed by using the proposed shading system. • In such an application of PCM, the MT of PCM has a negligible impact on the energy consumption of the building. • The system is not effective in winter and requires more research for PCM incorporated shading systems, according to the authors.
[38]	RT27 paraffin (27)	Cfa	E	DGW	Cooling and heating	• Using water instead of air in DGWs brings more temperature damping, but less favorable average temperature, which using PCM covers the latter issue.
[39]	n-eicosane (37)	-	N	DGW	Cooling	• PCM is placed between the frames of the DGW containing air between the panes. • Expanding the air gap to 40mm decreases the Nusselt number by 44%. • Decrease in heat transfer effectiveness was also observed due to PCM overheating
[40]	Different PCM variables (20, 30, 40, 50)	Warm, mixed, and cold	N	DGW	Cooling and heating	• A DGU's inside glass is coated with solid–solid translucent PCM. • 3 mm PCM integration causes 9.4%, 6.7%, and 3.2% building energy savings reduction in warm, mixed, and cold climates, respectively.
[41]	Paraffin wax	-	N	Glazing window	-	• TiO_2 nanoparticles in PCM for optical and thermal performance tests. Increasing nanoparticle diameter from 10 to 30 nm boosts nanoPCM scattering by 27.8 times.
[42]	Paraffin MG29 (27–29)	Cfa	E, N	TGW	Cooling and heating	• Triple-glazed window filled with PCM in the outside gap cavity space can avoid overheating phenomenon effectively. • In a typical sunny summer day, the PCM-TG window consumes 21.30% and 32.80% less energy than the PCM-DGW and hollow TGW, respectively

Table 3. *Cont.*

Ref.	PCM Type (MT °C)	Climate Code	Study Type	Envelope Element	Application	Findings and Remarks
[43]	Paraffin wax (18, 22, 25, 28. 31)	Dfb	E, N	TGW	Cooling	• PCM filled the outer cavity space of the glazing system, while Argon gas was used to fill the interior cavity space. • There is no optimum unit type of PCM for the system, and adopting PCMs with varying MTs is advantageous from an energy and optical standpoint, as liquid PCM provides a superb view of the sky and visual comfort, whereas solid PCM does not.
[44]	(25–28)	Dwa	E, N	FGW	Heating	• As a trade-off between maximizing the thermal comfort enhancement and minimizing the solar transmittance reduction, PCM thickness should not be larger than 20 mm.

As stated above, one of the primary difficulties that must be addressed when constructing latent storage added fenestrations systems is the PCM-GU system overheating. As a possible option despite using TGU- and QGU-PCM systems, the Prisma solar glass has been studied. Kara and Kurnuc [45] conducted an experimental investigation in Erzurum, Turkey (Dfb) during the summertime using Prisma solar glass combined with PCM and low-e glass in TG windows. In summer, the solar transmittance of the south-facing TG system was reduced by 100% compared to winter. They also observed that the PCM wall with Prisma solar glass did not warm throughout the summer. Later, Souayfane et al. [46] undertook a numerical and experimental investigation to assess the thermal performance of a super-insulated translucent wall (a triple glazing (TG) system) made of Prisma solar glass, silica aerogel, glass bricks filled with a fatty acid, and eutectic PCM. Figure 12 displays the translucent wall for the solid and liquid states of PCM. The experiment took place over the course of seven consecutive summer and winter days. The authors examined five distinct climates, including those of Madrid, Spain (Csa), Paris, France (Cfb), Chicago, USA (Dfa), Ottawa, Canada (Dfb), and Kiruna, Sweden (Dfc). Utilizing Prisma solar glass as opposed to conventional glasses has proven to be highly beneficial, since it eliminates the overheating issue in summer and maintains the system's benefits in winter. In addition, they assessed the necessity for ventilation systems and shade devices in the regions under consideration. Another method to avoid overheating is using laminated glasses. In a numerical and experimental investigation, Maduru and Shaik [47] examined the thermoeconomic and optical analyses of various laminated glazing for buildings. The authors used Ethylene vinyl acetate (EVA) films coated with a variety of tints, including transparent film, cooling film, scarlet red film, fabric film, Tiffany Blue film, Mist Rose film, and reflective film, as an interlayer between two transparent glass sheets, as shown in Figure 13. The reflective film laminated glass demonstrated the greatest solar heat gain reduction, annual cost savings, and CO_2 emission reduction. Additionally, the payback period of EVA films was studied, and it was determined that all had an initial payback cost of less than two years. The authors also evaluated the average daylight factor of the EVA films, indicating that it was above the minimum recommended level (0.625% in Indian standards), and that the EVA films allowed daylight into the buildings without glare.

Incorporating PCM-DGUs appears to be a potential technique for enhancing thermal comfort, reducing energy consumption, and decreasing temperature swings, however it reduces the glazing unit's optical performance or solar transmittance to the point where a trade-off is necessary. The thickness of the PCM should not exceed 16 to 20 mm as a result

of such a trade-off by researchers. In regions with greater solar heat gain (like areas whose code ends with "a"), PCM performs better. In addition, during the summer and when the sky is clear (which is more prevalent in areas whose code begins with "B"), PCM is more effective, whereas its performance in the winter and on cloudy days is questionable, necessitating the implementation of other passive and active techniques such as night ventilation. The volume expansion of the PCM during phase transition is an additional issue that must be considered. Another potential issue that has been discussed is the low solar transmittance of PCM solid phase compared to liquid phase. Utilizing solid–solid translucent PCM, which can also eliminate leakage and volume-changing difficulties, is one approach to circumvent this issue.

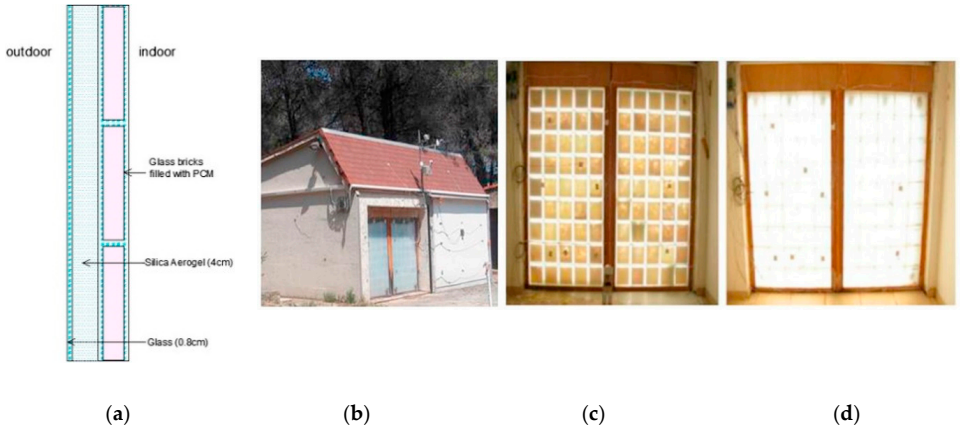

Figure 12. (**a**) Insulated translucent wall components, (**b**) outside view, and inside view in (**c**) solid and (**d**) liquid phases of the PCM [46].

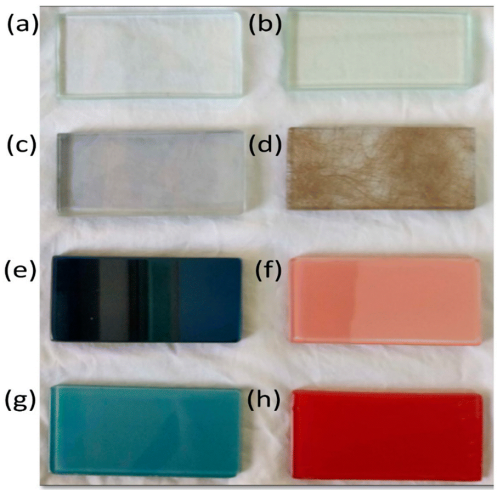

Figure 13. Laminated glass samples showing: (**a**) monolithic clear glass (6 mm), (**b**) transparent film, (**c**) cooling film, (**d**) fabric film, (**e**) reflective film, (**f**) Mist Rose film, (**g**) Tiffany Blue film, and (**h**) scarlet red [47].

3.1.2. PCM-Incorporated Shading Systems of GUs

Using shade devices within and outside the fenestration system (e.g., window) and between the panes of a multi-layered GU is one method for blocking solar heat from entering the interior environment. Numerous researchers are interested in using PCMs to boost the thermal mass and heat storage of shading devices. As an example, the use of PCM on internal shading devices was studied by Helmut et al. [48] as they compared the heating and cooling energy performance of an internal blind system incorporated PCM vs. the typical sun protection systems for a DG window in an experimental study conducted

in Bayern, Germany (Cfb). The blind system consisted of a hollow polycarbonate blind (12 mm gap) filled with encapsulated salt hydrate PCM with MT between 26 and 30 °C and sealed at the ends seen in Figure 14. The outcomes demonstrated that the PCM-integrated blind system significantly improves thermal comfort. The most significant issue, however, is the nighttime discharge of the PCM. Later, Wang and Zhao [49] carried out a numerical parametric research of PCM embedded into the curtain of residential buildings in Shanghai, China (Cfa), during the warmest days of the year. The air gap between the PCM curtain and the window was parameterized, as was the PCM MT. Consequently, other PCMs were evaluated, including paraffin with MTs of 28 °C, 29 °C, and 30 °C, and n-Eicosane with an MT of 37 °C. The scientists concluded that employing a 15 mm PCM layer with an MT of 29 °C reduces the average indoor heat transfer rate by 30.9%. In addition, the authors suggested a cascaded PCM layer with many MTs in a vertical orientation for future research to counteract the PCM curtain's disadvantage, which is the loss of window transparency due to the addition of an opaque layer.

Figure 14. Polycarbonate blinds filled with encapsulated salt hydrate PCM sealed at ends [48].

The use of PCM on shutter windows was studied by Silva et al. [50] as they performed an experimental setup of window shutter (hollow aluminum blade) filled with PCM (macro-capsulated) in the Mediterranean climate of Aveiro, Portugal (Csb) during the winter season (ambient air temperature between 4.5 °C to 14 °C). The organic PCM of paraffin RT28HC with MT of 27–29 °C was utilized in this study. The authors also benefited from a thermal camera (Testo®875i) to identify the test room's thermal bridges and heat losses (Figure 15). The obtained results proved that the maximum indoor temperature with PCM on shutter windows decreases by up to 30% compared to non-PCM shutter windows. Moreover, the energy efficiency enhancement and indoor spaces' thermal regulation were achieved by incorporating PCM into the DG window shutter blades. In a further experimental study, Silva et al. [51] examined the same issue during the summer (ambient air temperature ranging from 13 °C to 25 °C). The researchers determined an improvement of 18–22% in the thermal regulating capacity of interior temperature and a reduction of 6% and 11%, respectively, in the highest and minimum temperature peaks. Another similar study was performed by Silva et al. [52] to numerically simulate the thermal behavior of window shutters containing PCM (RT28HC) validated by real-scale test cells during the summer of 2013 (between the 2nd and 9th of August). The simulation was based on a 2D model analyzed with ANSYS Fluent software. Using a PCM-shutter window lessens the highest indoor temperature by up to 8.7% and increases the minimum indoor air temperature by 16.6% during the nighttime.

Considering using external shading devices, Park et al. [53] conducted numerical research in Seoul, South Korea (Dwa), to examine the energy performance and thermal comfort of an existing educational facility with a PCM-incorporated exterior shading system. As micro-packed PCMs for the shade system, the authors chose n-octadecane (NO) with an MT of 25.05–26.11 °C, n-eicosane (NE) with an MT of 33.63–35.64 °C, and n-docosane (ND) with an MT of 42.21–43.15 °C. Their technology reduced cooling energy consumption by 44% and increased thermal comfort hours by 34%. In addition, they argued

that in such an application of PCM, the MT of PCM has a negligible impact on the energy consumption of the building. In addition, they underline the need for additional research on PCM-integrated shade devices, as they discovered that the system could not be defeated throughout the winter.

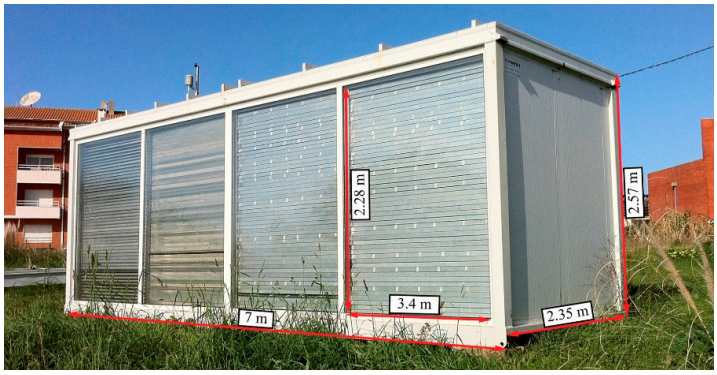

Figure 15. Test rooms' outside view including shutter windows [50–52].

The application of PCM on the shading devices between the panes of multi-layered GUs was examined by Li et al. [54] as they evaluated the thermal performance of a double skin facade (DSF) featuring a PCM-incorporated (as a microencapsulated coating) blind system between the two panes of the fenestration system using computational and empirical methods. Figure 16 depicts an experimental setting in Ningbo, China (Cfa). The simulations were carried out utilizing ANSYS Fluent software. The blind system incorporated the PX35 PCM with an MT of 35 °C. The results indicated that the air temperature in the DSF test cell did not exceed 39 °C for the entire day and was below 35 °C (the PCM's MT) before 10:00 and after 15:00, allowing the PCM blind system to undergo a complete solidification process. The researchers also argued that a decrease of 2.9 °C between the interior surface temperature of the DSF and its exterior surface temperature indicated a reduction in heat transfer through the building envelope. As indicated in Figure 17, Hu et al. [55] suggested a new fenestration system, incorporating a vented TG window with internal shade between the two inside panes and a PCM heat exchanger beneath the window for precooling and preheating purposes to conserve building energy. The research was carried out numerically with EnergyPlus software and experimentally in Denmark (Cfb). The authors opted for a PCM composed of fiber (50%) and paraffin wax (50%) with a freezing point of 20.7 °C. The proposed system increases energy savings by 62.35% and 9.4% in the summer and winter, respectively. Table 4 provides a summary of the reviewed research on PCM-integrated shading solutions for GUs.

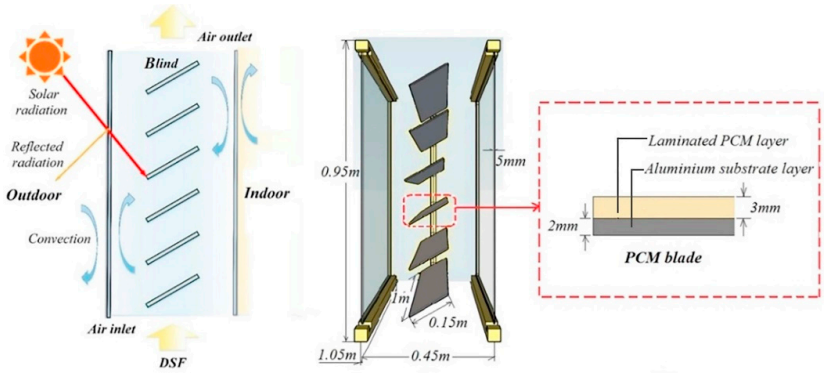

Figure 16. Schematic of experimental setup by Li et al. [54].

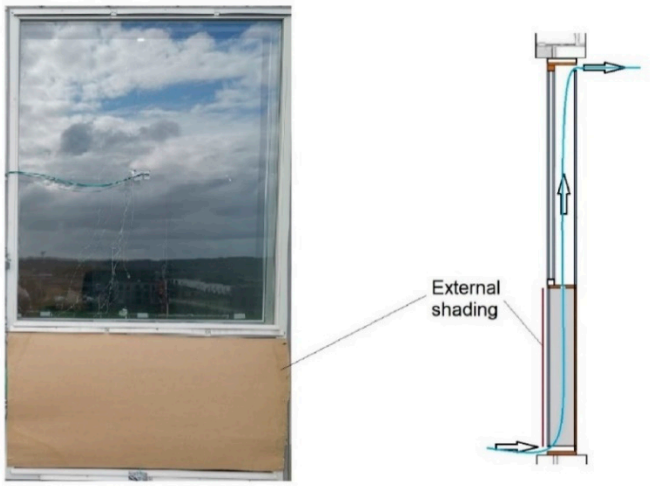

Figure 17. Outside view and components of the system proposed by Hu et al. [55].

Different PCM types have been incorporated into the interior, between, and exterior shading systems of GUs. Utilizing blinds with PCM has been demonstrated to reduce energy consumption and improve thermal regulation, albeit with some limits. When the blind system is located on the interior side of the GUs (the majority of research are conducted in countries with temperate climatic conditions, where the code begins with "C"), the absorbed heat during the day must not be released to the inside, requiring nighttime ventilation. In winter, however, it absorbs heat during the day and releases it inside, which is a favorable effect, but it filters more sunlight during the day due to the addition of opaque material to the blind system. To prevent the loss of sunlight, a cascaded PCM integration with several MTs is suggested. When the blind system is located on the outside side of the GUs, the MT of the PCM has a subtle influence on energy savings, which is beneficial in the summer but not in the winter, indicating the need for additional research. Using PCM between the panes exhibits promising thermal storage of the latent system during the summer's hottest days. To potentially utilize the temperature regulation enhancing benefits of PCM-incorporated shading systems, this topic has been researched infrequently and requires additional investigation.

Table 4. Summary of PCM-incorporated shading systems of GUs.

Ref.	PCM Type (MT °C)	Climate Code	Study Type	Shading Position of the GU	Application	Findings and Remarks
[48]	Salt hydrate (26–30)	Cfb	E	Interior	Cooling and heating	• A hollow polycarbonate blind (12 mm gap) was filled with PCM. • The sun protection system improves thermal comfort. The most significant issue, however, is the nighttime discharge of the PCM.
[49]	Paraffin (28, 29, 30) n-Eicosane (37)	Cfa	N	Interior	Cooling	• The average heat transfer rate is reduced by about 31% by using a 15 mm PCM layer on the hottest summer days. • The authors suggested a cascaded PCM layer with many MTs to avoid the loss of window transparency due to the addition of an opaque layer.

Table 4. *Cont.*

Ref.	PCM Type (MT °C)	Climate Code	Study Type	Shading Position of the GU	Application	Findings and Remarks
[50]	Paraffin RT28HC (27–29)	Csb	E	Interior	Heating	• Incorporating PCM into shutter window (hollow aluminum blade) increases 30% reduction in maximum indoor temperature compared to the system without PCM.
[51]	Paraffin RT28HC (27–29)	Csb	E	Interior	Cooling	• The PCM sun protection system causes an enhancement in the thermal regulating capacity of the indoor temperature by about 18–22%.
[52]	Paraffin RT28HC (27–29)	Csb	N	Interior	Cooling	• PCM-shutter window lessens the highest indoor temperature by up to 8.7% and increases the minimum indoor air temperature by 16.6% during the nighttime.
[53]	*n*–octadecane (25.05–26.11) *n*-eicosane (33.63–35.64) *n*-docosane (42.21–43.15)	Dwa	N	Exterior	Cooling and heating	• 44% reduction in cooling energy consumption and 34% improvement in thermal comfort are observed by using the proposed shading system. • In such an application of PCM, the MT of PCM has a negligible impact on the energy consumption of the building. • The system is not effective in winter and requires more research.
[54]	PX35 as an organic PCM (35)	Cfa	E, N	Between the panes	Cooling	• The PCM shading system keeps the average temperature below 35 °C between the panes of the DGU during the summer, with testing showing subtle differences with ambient temperature.
[55]	mixture of fiber and paraffin (20.7)	Cfb	E, N	Between the panes	Cooling and heating	• Using a PCM-contained chamber beneath the shading system for preheating and precooling purposes. 62.35% and 9.4% enhancement in energy saving is observed for the proposed system in summer and winter, respectively.

3.1.3. PCM/PV-Incorporated Multi-Layered GUs

Researchers have recently implemented the use of PCM materials as the sensible and latent heat storage and PV layer as the electricity generation in fenestration systems. Elarga et al. [56] numerically evaluated the optical, electrical, and thermal performance of a PV-PCM in DSFs. These systems were tested in Venice, Italy (Cfa), Helsinki, Finland (Dfb), and Abu Dhabi, United Arab Emirates (Bwh). The authors utilized RT42-Organic PCM for Venice and Helsinki, RT55-Organic PCM for Abu Dhabi, and an a-Si (amorphous Silicon) thin-layer solar cell for the PV layer. The combination of a PCM layer and a semi-transparent PV layer within the space cavity of the DSF raised monthly energy savings by 20–30%, independent of climate. The scientists observed that the selection of PCM material with the appropriate MT and a ventilation plan are the primary factors that have contributed to an efficient thermal and energy conversion system. Maintaining the PCM material at its mushy zone or phase transition allowed for the greatest thermal performance. This can be

accomplished by installing a ventilation system that protects the PCM from overheating and overcooling. In a separate numerical work, Elarga et al. [57] simulated and optimized (using a genetic multi-optimization technique) a forced-ventilated PV-PCM integration in DSF and TSF systems. For their numerical simulations, they employed a 1D model and the finite difference method. In the DSF system, the PV module was placed in the cavity area between the panes, but in the TGF system, the PCM was placed on the outside surface of the middle pane and the PV module was placed on the outer surface of the PCM. The optimal scenario reduces thermal loads by 26.4%. The authors suggested 2D simulations to capture the likely occurrence of stratification effect in the higher altitude façade and energy cost as part of the optimization strategy for the PV-PCM DSF system for further research. Ziasistani and Fazelpour [58] assessed the thermal and energy performance of a building with various glazing types of a DSF combined with a PV layer coated on the outside skin and inserting PCM to the walls using the DesignBuilder. These researchers evaluated six varieties of glazing, including single and double layers. As the PV layer, they chose monocrystalline silicon PVs. All major building orientations were evaluated in six Iranian cities: Tehran (Bwh), Tabriz (Bsk), Shiraz (Bwh), Esfahan (Bwh), Bandar Abbas (Bwh), and Yazd (Bwh). They demonstrated that west- and north-facing DSF result in the highest energy usage and the lowest cooling load, respectively. With the exception of Bandar Abbas (Bwh), the highest yearly electricity generation was also found with an orientation of 180 degrees in all cities. Heydari and Khoshkhoo [59] analyzed the energy performance of a six-story structure in four Iranian cities, namely Rasht (Cfa), Tabriz (Bsk), Yazd (Bwh), and Bandar Abbas (Bwh), by adopting DSF with PV layer on the external pane and PCM on the walls. The investigation was numerically simulated using the software package DesignBuilder. They demonstrated that the air cavity depth in DSF has a slight impact on the cooling and heating loads of buildings in every city tested. The overall energy production by the PV module for all orientations in Yazd, Bandar Abbas, Tabriz, and Rasht was reported to be 52.56, 44.49, 36.87, and 33.48 MWh, respectively. Using PCM in the walls had a negligible impact on energy consumption, as the PCM's phase change cycle did not occur throughout the study period (from 7:00 to 19:00). Ahmed et al. [60] incorporated four technologies for sliding smart windows, including air-gap, PCM, PV, and vacuum glazing for the climatic condition of Kuwait city (Bwh) in Kuwait. Figure 18 shows the glazing systems modelled by the authors. The researchers demonstrated that the presence of PCM in fenestration systems alters the PV system's safe operation and the peak indoor heat gain. The full example (Figure 18e) with a mechanically forced ventilation system was determined to be the optimal scenario for the efficient functioning and thermal insulation of the PV system. Future efforts proposed by the authors include long-term simulations involving the observation of the phase change cycle the PCM undergoes in a 24-h period, as well as varying weather conditions. Ke et al. [61] presented a multi-layer ventilated window with a PV layer (cadmium telluride or CdTe cell) combined with a PCM layer, with MT of 27–29 °C and 18–20 °C for summer and winter seasons, respectively, in the middle layer for Hefei, China's climatic conditions (Cfa). Using PCM, they determined an improvement in the electrical efficiency of the PV window and an increase in the thermal comfort of the interior. Among climatic parameters, it was discovered that the thermal and electrical performance of the system is most sensitive to ambient temperature and solar heat gain. In addition, the authors recorded a 1246.87 kWh reduction in air conditioning demand. Figure 19 depicts the PCM-PV multi-layer ventilated window in summer and winter modes. Table 5 provides a summary of the reviewed research on PCM-integrated shading solutions for GUs.

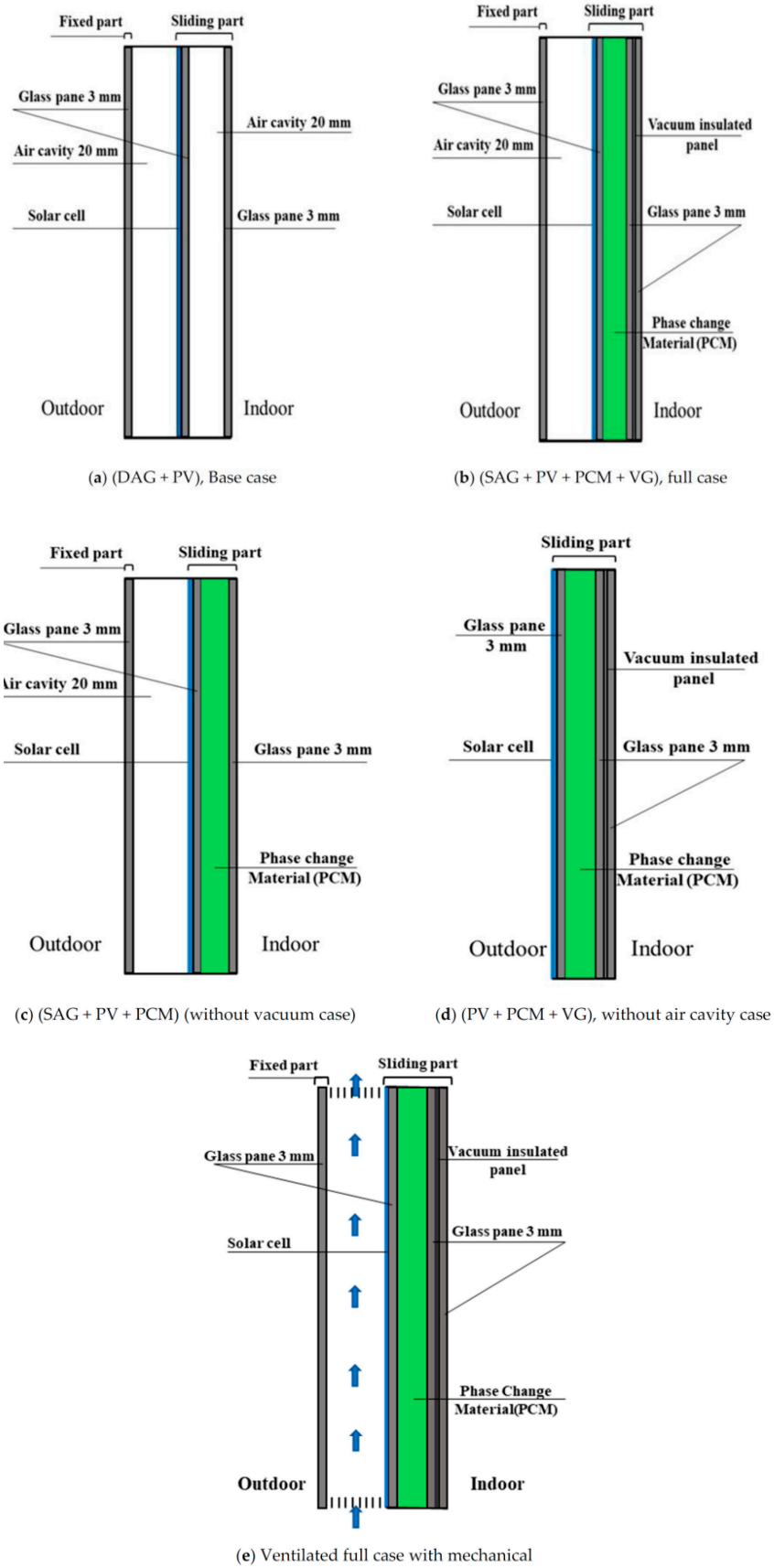

Figure 18. Different proposed windows by Ahmed et al. [60] showing: (**a**) base case, (**b**) full case, (**c**) without vacuum case, (**d**) without air cavity case, and (**e**) mechanical ventilated full case.

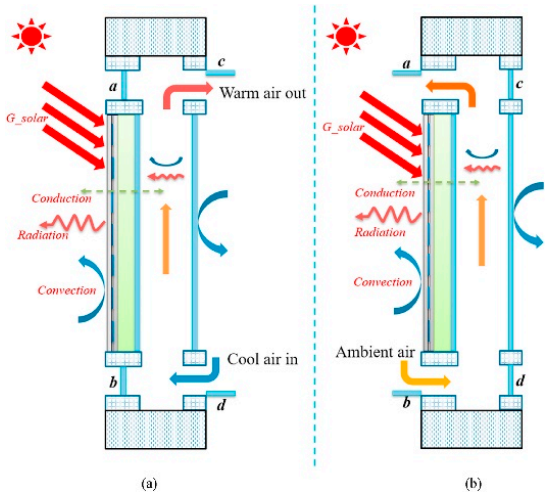

Figure 19. Energy flow and operating modes of the PCM-PV multi-layer ventilated glazing system in (**a**) winter mode and (**b**) summer mode, listed as vents a, b, c, and d [61].

Table 5. Summary of PCM/PV-incorporated multi-layer GUs.

Ref.	PCM Type (MT °C)	Solar Cell Type	Climate Code	Study Type	Application	Findings and Remarks
[56]	RT42 (42) RT55 (55)	a-Si	Cfa, Dfb Bwh	N	Cooling and heating	• The proposed system causes a 20–30% increase in the monthly energy saving, regardless of the climate. • Installing a ventilation system along with an appropriate MT for PCM is necessary to maintain the PCM in mushy zone to avoid overheating and overcooling.
[57]	RT35 (35)	a-Si	-	N	Cooling and heating	• PV-only layer is applied to a DGU, and PV-PCM layer is applied to a TGU. • The optimum case leads to a 26.4% reduction in thermal loads.
[58]	BioPCM -M182/Q25 (25)	monocrystalline silicon	Bwh BSk,	N	Cooling and heating	• PV layer is applied to a DGU, and PCM is applied to the walls. • West-faced and north-faced DSF lead to maximum energy consumption and minimum cooling load, respectively.
[59]	BioPcm-Q23 (23)	a-Si	Cfa, Bsk, Bwh	N	Cooling and heating	• PV layer is applied to a DGU, and PCM is applied to the walls. • Air cavity depth in DSF has a subtle effect on the cooling and heating loads of the buildings in all studied cities. • From 7 am to 7 pm, the use of PCM in walls has an insignificant effect on energy consumption as during the hours, the phase change cycle is not complete.

Table 5. *Cont.*

Ref.	PCM Type (MT °C)	Solar Cell Type	Climate Code	Study Type	Application	Findings and Remarks
[60]	RT35HC (34–36)	Silicon wafer	Bwh	N	Cooling	• The presence of PCM in the fenestration systems causes the PV module to operate safely and the peak indoor heat gain to be shifted.
[61]	(27–29) for cooling (18–20) for heating	CdTe	Cfa	N	Cooling and heating	• 1246.87 kWh saving in the air-conditioning load is reported. • Thermal and electrical performance of the system is mainly sensitive to ambient temperature and solar heat gain among the weather factors.

Using a PV layer in conjunction with a PCM layer in the glazing units appears to be a promising technology that requires further investigation to fully exploit the utilization of combined PCM-PV technology. The PCM ensures the safe operation of the PV module, which improves the thermal performance of the smart glazing system. In addition, establishing a ventilation system to prevent PCM from overheating or overcooling is suggested. As the PV layer restricts sunlight transmittance, it might be utilized to prevent the PCM from overheating in addition to producing electricity. In these systems, ambient temperature and solar heat gains influence thermal and electrical performance the most.

3.2. Technologies of GUs without PCM Utilization

3.2.1. Photovoltaic (PV) Window

The sole use of the PV layer in fenestration systems, often known as a PV-window, has recently captured the interest of numerous researchers. Cuce et al. [62] developed a multi-functional glazing technology known as high insulation solar glass (HISG), which can not only generate electricity like conventional PV panels by having an amorphous silicon PV module, but can also provide thermal and acoustic insulation, energy savings, and self-cleaning due to the presence of a nano-coating known as TiO_2. The test rooms were done in Taiwan (Cfa), as shown in Figure 20. The authors calculated that the HISG delivers 100% UV blockage, which is beneficial to human health. HISG generates 16% more electricity than conventional PV glazing due to the nanolayer reflective film included therein. In addition, the HISG shading coefficient was reported to be 0.136, indicating an almost 80% reduction in solar heat gain compared to standard glass. In addition, the energy savings for heating and cooling seasons employing HISG were observed to be 38% and 48%, respectively. Sharma et al. [63] designed a PV-TSF by adding a perforated metallic sheet into the cavity space of a PV-DSF system in order to remove the heat from the pans' space cavity with minimal restriction of sunlight entering the building and to benefit from natural ventilation in the cavity. Figure 21 depicts the inside and exterior perspectives of the window system used by the authors. In an experiment done in Jaipur, India (Bsh), the authors also evaluated the system's thermal and electrical performance. The researchers concluded that applying the perforated sheet with 60% perforation decreases the solar heat gain coefficient by approximately 14.7% compared to the PV-DSF system with a cavity distance of 200 mm. In general, they determined that PV-TSF is superior to PV-DSF because the former does not require a wide air gap between the panes. Tang et al. [64] suggested a new DG-PV curtain wall system paired with an air handling unit based on exhaust cooling and heating recovery, as seen in Figure 22, in order to evaluate its electrical and thermal performance. A numerical simulation was conducted for a typical summer week operating in Hefei, China (Cfa). Using the proposed PV system for the curtain wall reduced the building's total energy consumption by 19.26%. Furthermore, it was discovered that a 0.08 m depth

for the air cavity and a greater PV coverage ratio resulted in a greater energy-saving potential, making the system a viable choice for green technology. Luo et al. [65] studied the energy performance of a double skin façade (DSF) using PV-blinds (PVBs) as a shading device placed to the façade inside surface of a south-facing wall through a numerical and experimental analysis. They utilized amorphous silicon (a-Si) for the PVB system's solar cell. The PVB-DSF system generates power, mitigates solar transmittance, and provides adjustable daylighting management. The experimental site was constructed during frigid winters and hot summers in Changsha, China (Cfa), which has a climate that is warm and moderate. The angle and space of PVB were investigated using a parametric model. In comparison to a typical DSF without shading devices and one with shading devices, their proposed system might save around 12.16 and 25.57 percent of energy during the summer months. They also proposed that the PV-DSF system must use natural ventilation mode throughout the summer. Tan et al. [66] explored a four-layer PV-integrated DGU, commonly known as vacuum-PV glazing, using numerical and experimental methods. To enhance the power generation of the PV module, the authors positioned the CdTe laminate and DG on the external and indoor sides, respectively. The vacuum PV glazing unit has a U-value of 0.89 W/m^2K, according to the researchers' numerical findings. The study was conducted in various Chinese cities, including Harbin (Dwa), Beijing (Dwa), Changsha (Cfa), Guangzhou (Cwa), and Kunming (Cwb), where the proposed PV-window produced average yearly power outputs of 47 kWh/m^2, 48 kWh/m^2, 34 kWh/m^2, 36 kWh/m^2, and 45 kWh/m^2, respectively. The components of the PV glazing system utilized by the authors are illustrated in Figure 23. Uddin et al. [67] presented PV combined hybrid vacuum glazing as a new technique in comparison to PV combined vacuum glazing, which has been less investigated. Figure 24 depicts the CdTe-based semitransparent PV window system construction. According to reports, the U-value of the proposed system is 1.145. The authors investigated the energy performance of the suggested glazing system in five climate conditions in China, namely Hohhot, Inner Mongolia (Bsk), Tianjin, Tianjin (Dwa), Hefei, Anhui (Cfa), Kunming, Yunnan (Cwb), and Xiamen, Fujian (Cwa). The authors noted that the suggested glazing system lowers energy consumption by roughly 59.5% and 40% in cold climate regions and 76.5% and 74% in hot climate regions when compared to single clear glazing and DG windows, respectively. Wang et al. [68] carried out a numerical and experimental study to examine the annual energy performance of a ventilated DGW integrated with CdTe PV cells. They showed 25% to 30% of the annual electrical loss was attributable to the extinction and reflection of the glass. It was also found that increasing the PV coverage proportion causes the net energy consumption of the three cities (i.e., Hefei (Cfa), Harbin (Dwb), and Haikou (Cwa) in China) to initially fall and subsequently rise. Optimum PV coverage proportion for minimum net energy consumption was reported as 50%, 60%, and 70% for Harbin, Hefei, and Haikou, respectively. Alrashidi et al. [69] performed an experimental study to assess the daylight control, energy saving, and power generation of PV-DGW using CdTe solar cells in Penryn, UK (Cfb). It was found that PV glass with the least amount of transparency can decrease solar heat gain by 96% and cooling energy by 23.2% when applied in a south-west orientation in comparison to standard clear glazing. Zhang et al. [70] numerically and experimentally examined the thermal and electrical performance of ventilated PV-DGW using CdTe solar cells in Hefei, China (Cfa). According to their results, the WWR and PV coverage of ventilated PV-DGW had a significant effect on the heat transmission and electrical output of the glazing system. Changes in the emissivity of low-e coating had no effect on the window's performance. Numerous researchers have recently demonstrated the potential application of PV layer in glazing systems [71–73], with cadmium telluride (CdTe) solar cells being the most prevalent in PV windows [74–78]. Su et al. [79] examined the energy and electrical performance of PVB systems by adopting four solar cells, including amorphous silicon (a-Si), cadmium telluride (CdTe), dye-sensitized solar cell (DSSC), and perovskite solar cell (PSC). The CdTe PV cell had the best performance among the four solar cells examined. Table 6 provides a summary of the relevant studies on PV window systems.

Figure 20. Example of high insulation solar glass system's outside view [62].

Figure 21. Inside and outside views of fenestration system proposed by Sharma et al. [63].

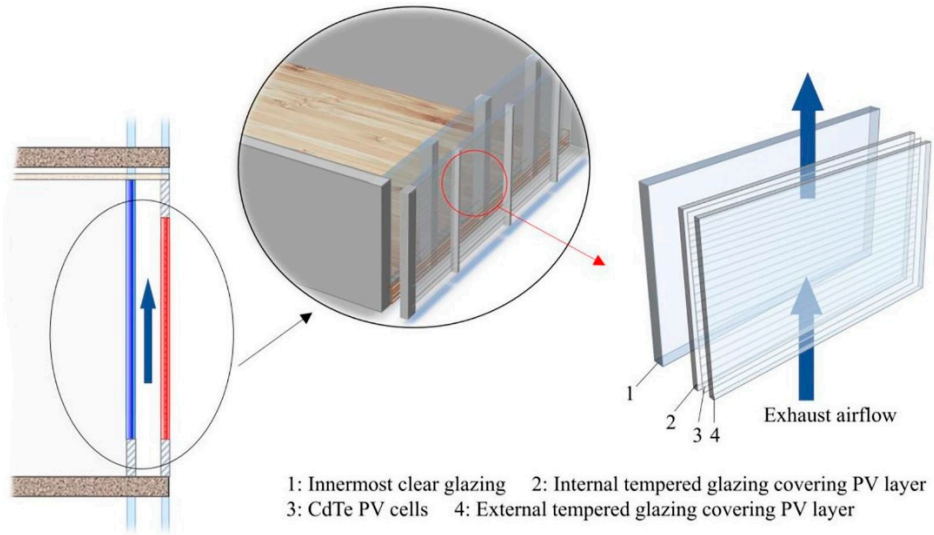

Figure 22. Proposed PV-incorporated DGU system by Tang et al. [64].

Table 6. Summary of PV window systems.

Ref.	Solar Cell Type	Climate Code	Study Type	Envelope Element	Application	Findings and Remarks
[62]	a-Si + TiO_2 nano-coating	Cfa	E	DGW	Cooling and heating	• The glazing system is self-cleaning due to the nano-coating and 100% UV protection. • 80% reduction in solar heat gain is reported compared to standard glass. • The energy savings for heating and cooling seasons employing the proposed glazing system are observed to be 38% and 48%, respectively.
[63]	CdTe	Bsh	E	DGW + a sheet	Cooling	• Implementing of the perforated sheet with 60% perforation reduces the solar heat gain coefficient by about 14.7% compared to the PV-DSF system with pane cavity distance of 200 mm.
[64]	CdTe	Cfa	N	DGW	Cooling	• 19.26% reduction in the overall energy consumption using the proposed PV system for the curtain wall.
[65]	a-Si	Cfa	E, N	DGW	Cooling and heating	• Energy saving in summer is about 12.16% and 25.57% compared to a conventional DSF without and with shading devices, respectively.
[66]	CdTe	Dwa, Cfa, Cwa, Cwb	E, N	DGW	Cooling and heating	• Average annual power output was reported as about 47 kWh/m^2, 35 kWh/m^2, and 45 kWh/m for climates with the classification codes Dwa, Cfa, and Cwb, respectively.
[67]	CdTe	Bsk, Dwa, Cfa, Cwa, Cwb	E, N	DGW	Cooling and heating	• The proposed glazing system saves energy consumption by about 59.5% and 40% in cold dominate climate regions and 76.5% and 74% in hot dominant climate regions versus single clear glazing and DG windows, respectively.

Table 6. *Cont.*

Ref.	Solar Cell Type	Climate Code	Study Type	Envelope Element	Application	Findings and Remarks
[68]	CdTe	Cfa, Dwb, Cwa	E, N	DGW	Cooling and heating	• Optimum PV coverage proportion for minimum net energy consumption is reported as 50%, 60%, and 70% for Dwb, Cfa, and Cwa, respectively.
[69]	CdTe	Cfb	E	DGW	Cooling	• PV glass decreases solar heat gain by 96% and cooling energy by 23.2% when applied in a south-west orientation in comparison to standard clear glazing.
[70]	CdTe	Cfa	E, N	DGW	Cooling and heating	• WWR and PV coverage of ventilated PV-DGW had a significant effect on the heat transmission and electrical output of the glazing system.
[79]	CdTe, a-Si, DSSC, PSC	-	N	DGW	Cooling and heating	• CdTe PV cell is reported as the best performance among the four studied solar cells.

According to the aforementioned literature, the use of solar cells to generate electricity from sunlight is a viable technology used to GUs to boost energy savings. It can be concluded that places with a greater amount of sunlight, such as those whose second letter code is "w", give greater energy savings through the use of PV layers in GUs. It is because certain places encounter less cloudy days in a year and more sunlight may reach the solar cell. Since PV-window technology alone has been employed more frequently than in collaboration with other smart glazing technologies and has demonstrated promising energy-saving performance, it might be integrated with other passive technologies to improve the thermal performance of smart glazing technology.

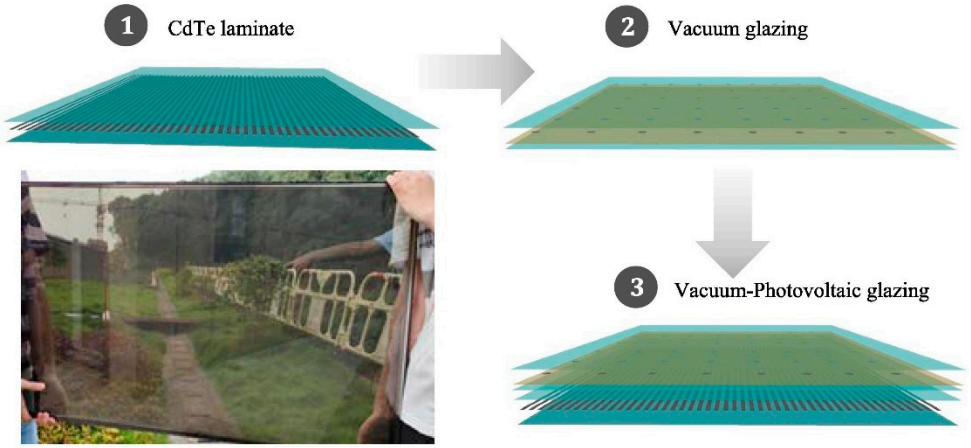

Figure 23. Example of PV-GU system components [66].

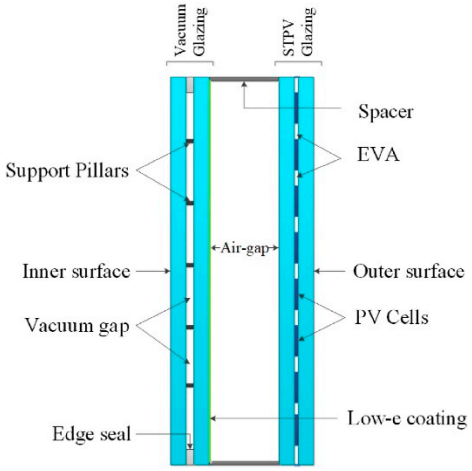

Figure 24. Example of PV combined hybrid vacuum glazing system [67].

3.2.2. Shading Systems (without PCM)

Various shading methods for indoor thermal comfort have been integrated into the window system to improve energy efficiency. Due to the use of external shading devices, Touma and Ouahrani [80] conducted an annual energy-saving research of brise soleil and venetian blinds applied to the outer face of a DGW on both north- and south-facing facades using EnergyPlus and experimentally validated their findings. The examination rooms were fully glazed offices in Doha, Qatar (Bwh). It was discovered that brise soleil and fixed blinds with 90° save the energy consumption by 18.6% and 20.6% annually in south-facing facades and 7.7% and 9.0% annually in north-facing facades. It was proved that the shading devices reduce glare risks on the south façade while eliminating the glare risks entirely on the north façade. Finally, they demonstrated that shade control can reduce energy use by 26.1%. Duttaa et al. [81] presented a sun-path-based autonomous movable outside shade device with multiple orientations for an annual energy-saving performance evaluation. In tropical wet and dry weather (Aw), the heat transfer from the sun to the window was greatest in the South, followed by the East, West, and North. Maximum energy savings in June were 14.9% and average annual savings were 9.8%, respectively. The authors also claimed six months of financial payback for their proposed shading device. Fedorczak-Cisak et al. [82] examined the overheating risk reduction of highly glazed office rooms in Kraków, Poland (Dfb), during the transition season (spring) of a temperate environment, when air conditioning units are typically not operating. According to these studies, exterior shading blinds with a 45° angle reduce discomfort hours during working hours by 92% compared to a fenestration system without venetian blinds. Kuczyski et al. [83] compared the thermal performance of three passive cooling approaches, including night ventilation, thermal mass, and external blinds, in a building with a temperate climate in central-western Poland (Cfb). The authors discovered that night ventilation and an increase in thermal mass do not considerably reduce the number of hours in which the maximum temperature is exceeded, however closing the exterior blinds eliminates the problem. Carlier et al. [84] performed a numerical analysis of the annual energy performance of residential structures with switchable insulation systems (SIS) applied to windows as shades and outside walls as dynamic simulation. The climatic data for Brussels (Cfb), Oostende (Cfb), and St. Hubert (Cfb) in Belgium and Barcelona (Csa) in Spain were established for two types of homes, namely a single-family home and an apartment. The researchers argued that SIS-integrated windows eliminate the need for mechanical cooling and reduce heating energy consumption by 44% in Belgium. It was also noted that Belgium and Spain, with their milder temperatures, could profit from such a system, particularly in terms of energy savings for heating. The orientation of the windows and the behavior of the inhabitants were also identified as critical factors in SIS energy performance.

The internal use of shading devices also drew the interest of researchers. Wang et al. [85] presented a movable shade curtain inside and outside of a single-layer window in Beijing, China (Dwa) to numerically evaluate and experiment with its energy-saving performance throughout the year. They demonstrated that during the winter, the movable curtain may be rolled down at night to reduce heat loss and raised during the day to maximize solar heat gain through the window openings. They evaluated the position of the curtain (inside and outside), whether it was rolled up or down, the air gap distance between the window and curtain, the heat transfer coefficient, and the size of the window-to-wall ratio. The optimal example was determined to be one with a window-to-wall ratio of 0.26 and a heat transfer coefficient of 1.02 W/m^2, resulting in a 75% increase in annual energy savings. Additionally, the authors demonstrate that the suggested insulated windows result in more desired indoor temperatures, less heating, cooling, and annual loads, and a possible price-to-load ratio compared to existing energy-saving windows. Using infrared thermography images and building simulation, Cho et al. [86] studied the energy and hygrothermal performance of retrofitting a cultural property with various energy efficiency measure packages. The construction site was in Seoul, Korea (Dwa). Using EnergyPlus and WUFI models, energy and hygrothermal simulations of a building were simulated. The package of technologies, which included the replacement of TG windows with low-e coating, the addition of insulation, the improvement of airtightness, the installation of internal blinds, and the replacement of incandescent lighting with LEDs, reduced heating energy consumption by 72% and total energy consumption by 60%, respectively. Tan et al. [87] conducted a numerically and experimentally validated annual energy study of internal venetian blinds in residential structures. Positioned on the interior surface of a DG window as depicted in Figure 25, they evaluated various blind angles and shade states, namely fully opened, partly opened, and fully closed. This study utilized typical meteorological years for Houston (Cfa) and Minneapolis (Dfa) in the United States. According to the results, the results showed that the two most influential parameters on annual energy performance are (i) solar transmittance, (ii) solar reflectance, and (i) thermal infrared transmittance, (ii) inner emissivity for cooling-dominated and heating-dominated climates, respectively. It was stated that cooling and heating energy savings might be reduced by 44% and 65%, respectively. Additionally explored were shading devices between multi-layered windows.

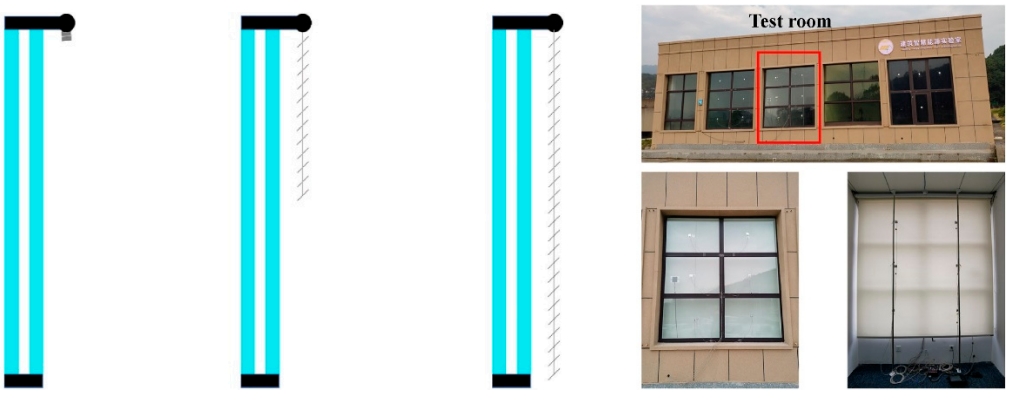

Figure 25. The outside view of the test room, along with the position of the shading devices [87].

Zhang et al. [88] experimentally studied and dynamically modelled a TG exhaust air window, combining adjustable venetian blinds within the window. As illustrated in Figure 26, the blinds were positioned between the external and middle panes to be fully opened in summer mode and entirely closed in winter mode. In addition to movable shades, they profited from switchable components that facilitated the summer and winter modes' exhaust air flow. On a typical summer day in Wuhan, China (Cfa), which has a humid subtropical climate, the effects of airflow velocity within the TG window and

blinds angles on the system thermal performance were examined. The authors say that the switchable exhaust air window is suitable in both newly constructed and retrofitted buildings since it greatly reduces cooling and heating loads, as well as peak loads, resulting in lower beginning costs for air-conditioning systems. Table 7 provides a summary of the researched literature on shading systems without PCM.

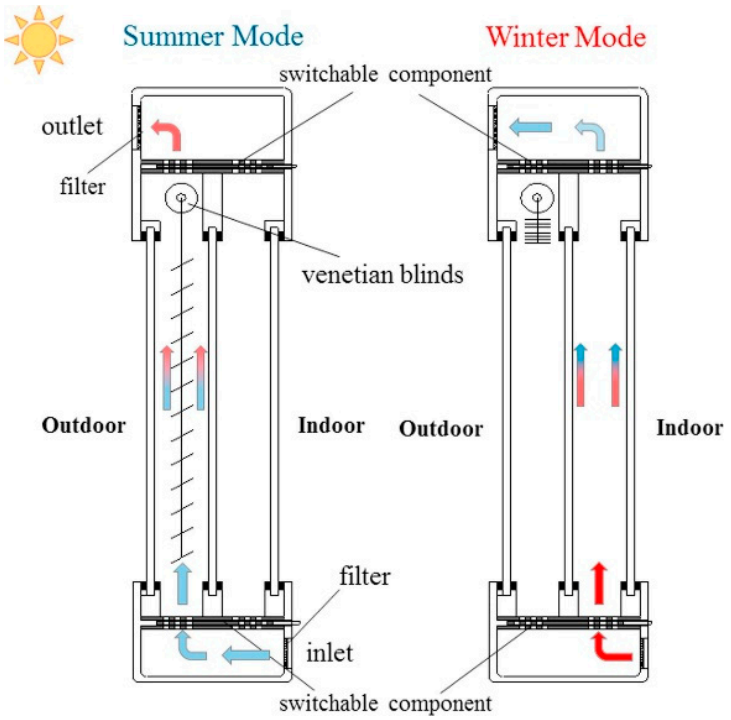

Figure 26. Example of blind position and air flow in winter and summer modes [88].

Table 7. Summary of shading systems (without PCM).

Ref.	Climate Code	Study Type	Shading Position of the GU	Application	Findings and Remarks
[80]	Bwh	E, N	External	Cooling and heating	• South-facing facades with shading devices reduce energy usage more than north-facing ones. Utilizing shade control has been shown to reduce energy consumption by 26.1%.
[81]	Aw	E, N	External	Cooling and heating	• 14.9% and 9.8% energy savings were reported as the maximum savings in June and for an average annual saving, respectively. The authors also claimed six months of financial payback for their proposed shading device.
[82]	Dfb	E	External	Cooling spring	• External shading blind with an angle of 45° results in 92% reduction in discomfort hours during working hours compared to a fenestration system without venetian blinds.
[83]	Cfb	E	External	Cooling	• Night ventilation and an increase in thermal mass do not considerably reduce the number of hours in which the maximum temperature is exceeded, however closing the exterior blinds eliminates the problem.

Table 7. *Cont.*

Ref.	Climate Code	Study Type	Shading Position of the GU	Application	Findings and Remarks
[84]	Csa, Cfb	N	External	Cooling and heating	• Using switchable insulation systems applied to windows as shades causes no use of mechanical cooling and 44% decrease in heating energy end-use in Belgium (Cfb). • The studied regions could profit from such a system, particularly in terms of energy savings for heating.
[85]	Dwa	E, N	Internal	Cooling and heating	• The optimum case is the one with window to wall ratio of 0.26 and heat transfer coefficient of 1.02 W/m^2, resulting in 75% enhancement of the annual energy saving.
[86]	Dwa	E, N	Internal	Cooling and heating	• The package containing all the studied technologies including installing internal blinds decreases 72% and 60% of the heating energy and total energy consumption, respectively.
[87]	Cfa, Dfa	E, N	Internal	Cooling and heating	• The two most influential parameters on annual energy performance are (i) solar transmittance, (ii) solar reflectance, and (i) thermal infrared transmittance, (ii) inner emissivity for cooling-dominated and heating-dominated climates, respectively. • The proposed system causes 44% and 65% energy saving for cooling and heating, respectively.
[88]	Cfa	E, N	Between the panes	Cooling and heating	• The proposed switchable exhaust air TG window is applicable in a newly constructed building and retrofitting due to its energy-saving enhancement and peak load reduction benefits.

According to the above literature review, the smart shading system is a passive approach employed in GUs to improve thermal comfort and saving energy. The use of active strategies to optimize the operation of shade systems throughout the year has been discussed. The performance of such devices is strongly affected by the behavior of the occupants. However, further study is required to incorporate such systems with other passive techniques in order to achieve the desired energy savings.

3.2.3. Chromogenic (Thermotropic and Thermochromic) Materials in GUs

Chromogenic materials, including thermotropic and thermochromic materials, are valuable design tools for dynamically controlling solar energy heat transmission. Thermotropic materials change their light transmittance behavior reversibly from extremely transparent to light scattering, sometimes referred to as a turbid state, when the majority of light reflects outside at a temperature threshold known as lower critical solution temperature (LCST). As the temperature increases, the outer material alters its behavior to prevent sunlight transmission and overheating. Thermotropic effects studied in the solar control field can be induced by a phase separation process, a phase transition between an isotropic and an anisotropic (liquid-crystalline) state, and by very differing temperature dependences of the refractive indices of domains and matrices. Polymer mixtures and polymeric hydrogels have been widely researched. Thermochromic materials alter their visible optical characteristics as a function of temperature. Consequently, the integration of a sensor or actuator into the material itself is made possible. If the thermochromic material absorbs more light as the temperature rises, also known as positive thermochromism or inverse thermochromism, smart windows may be a viable use. This effect of moving from a

transparent, low-hued, or colorless state to a brightly colored one has already been proven by laboratory prototypes. In addition, the public has been shown samples of products that are ready for sale [89].

Pertaining to the use of thermotropic materials in smart glazing systems, Yao and Zhu [90] numerically investigated thermotropic windows of a typical six-story residential building located in Hangzhou, China (Cfa) to increase the energy efficiency, daylighting, and thermal performance of building envelopes. The researchers conducted their numerical calculations using the building modelling software DeST. The authors reported a 70% and 50% reduction in extremely uncomfortable indoor heat conditions when utilizing thermotropic DG west-facing windows as compared to DG windows and tinted DG windows, respectively. It was also discovered that the performance of the window system can be improved on east- and south-facing facades by selecting a thermotropic material with a lower LCST and a higher NaCl content. Therefore, the researchers suggested thermotropic material-based windows for thermal comfort, energy savings, and daylighting in hot summer and cold winter climatic building envelopes. Goia et al. [91] carried out an experiment to ascertain the energy performance of a south-facing TGU with a PCM layer and a thermotropic layer (n-alkane mixture) in Torino, Italy (Cfa), during the summer. According to researchers, inserting the PCM layer into the innermost cavity space of the TGU causes the PCM to remain longer in the mushy zone, resulting in a greater utilization of latent heat and a consequent improvement in the energy performance of the window system. The authors also demonstrated that the energy performance of the proposed glazing system is enhanced by the employment of thermotropic and PCM layers, as well as the simultaneous use of both technologies, and that inserting PCM at the innermost layer can accommodate a PCM layer with a lower nominal MT. Figure 27 demonstrates that Connelly et al. [92] utilized a thermotropic layer called Hydroxypropyl cellulose (HPC) polymer in a DGU, alongside a PV layer of an office building located in London, UK (Cfb). The authors investigated HPC concentrations ranging from 1% to 6%. The threshold temperature or transition temperature for 1 weight percent HPC and 6 weight percent HPC was reported to be approximately 44 °C and 40 °C, respectively. Below the transition temperature, the thermotropic material is in a translucent state (Figure 27a) with a reported reflectance of approximately 10%, whereas above the threshold temperature, the material is in a transparent state (Figure 27b) with a reported reflectance of approximately 70%. In general, the authors indicated that the HPC is a potential thermotropic material for the application of smart windows based on their empirical findings. Sun et al. [93] presented a numerical and experimental investigation to evaluate the energy and optical performances of a south-facing DG smart window employing transparent parallel slat insulation as a thermotropic material. The research was conducted in London (Cfb), Rome (Csa), Stockholm (Dfb), and Singapore (Af) under diverse environmental circumstances. The impact of the optical properties and transition temperature of the thermotropic material on the energy performance of buildings was evaluated. The authors reported a 27.1% increase in annual energy savings due to the usage of thermotropic metrical in the DGW against a standard DGW. Figure 28 depicts the thermotropic material with DGW incorporation in both its clear and translucent forms. In a separate study, Sun et al. [94] used the same smart glazing unit to quantitatively evaluate the thermal and optical performance of the unit on an energy building located in London, UK (Cfb). On the basis of the geometric features, i.e., slat spacing and slat tilt angle, and the thermotropic layer properties, i.e., temperature transient and optical properties, the thermal and optical performances of the building were analyzed. They determined that the suggested GU improves the building's energy performance by up to 22% in comparison to standard DGWs.

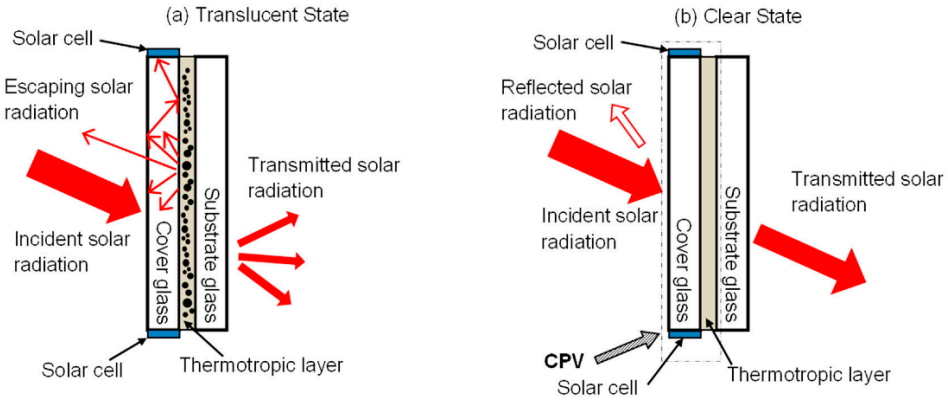

Figure 27. The thermotropic smart glazing along with PV layer in (**a**) translucent and (**b**) clear states [92].

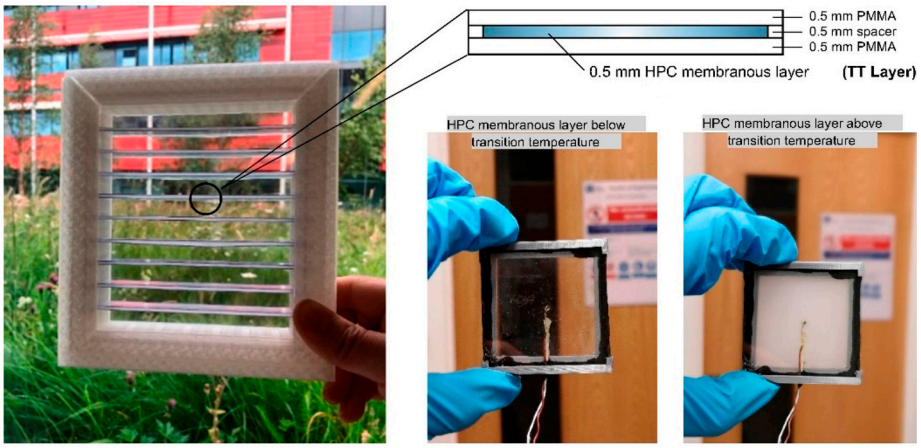

Figure 28. Photos of the DGW-incorporated thermotropic material in clear and translucent states [93].

Regarding the use of thermochromic materials, Long et al. [95] deployed a standard thermochromic material called vanadium dioxide (VO_2) coated into transparent portions and paraffin wax PCM into non-transparent parts of a building envelope to experimentally study the energy performance of a structure in Shanghai, China (Cfa). The phase change temperature of VO_2 thermochromic material was 41.3 °C, and the peak phase change temperature of the PCM was 38.8 °C. During the cooling period, the synergistic combination of PCM and VO_2 materials resulted in a higher level of thermal comfort than passive techniques alone, while simultaneously enhancing energy efficiency. Moreover, a negative ESI was achieved during the heating period, indicating a bad decision between using VO_2 alone and VO_2 and PCM together in cold regions. Then, Jin et al. [96] investigated the thermal performance of three passive approaches, including VO_2 thermochromic material, PCM, and low-e coating in DG and TG systems (shown in Figure 29) implemented in a building envelope in Shanghai, China (Cfa) using ANSYS Fluent software. The authors concluded that during the summer, the TG system with the three passive methods decreases the total heat gain compared to traditional DG windows by up to 32% on a sunny day and 40% on a cloudy day, whereas during the winter, the proposed system is not as effective as DGW due to the blockage of desirable solar energy. Ke et al. [97] developed a PCM-based aesthetic thermochromic window inspired by tetra-fish to improve the energy efficiency and aesthetics of a building. They utilized photonic co-doped VO_2 as the thermochromic layer exhibiting angle-dependent bright colors resembling the skin of tetra fishes. An office building in Beijing (Dwa), Hong Kong (Cwa), Bangkok (Aw), and Kuala Lumpur (Af) saved an additional 35.7 kWh/m^2 of energy annually, according to the results obtained. Tao et al. [98] conducted a CFD study in Shanghai, China (Cfa), to evaluate the optical and energy performance of six thermochromic materials with varying switching temperatures

ranging from 20 °C to 42.5 °C. As the maximum value for threshold temperatures between 25 °C and 35 °C, they observed a solar heat gain savings of 20.9%. Furthermore, the authors inferred that the optimal performance of thermochromic smart glazing occurs in places with long summer days and significantly lower solar radiation in winter days. Compared to thermotropic smart glazing, thermochromic smart glazing is of greater interest to the authors, and the majority of researchers have chosen VO_2 as the thermochromic layer [99–105]. Table 8 provides a summary of the research conducted on chromogenic materials.

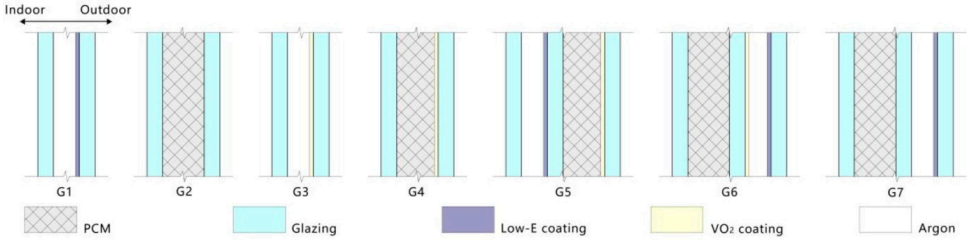

Figure 29. Different DG and TG systems used by Jin et al. [96].

Table 8. Summary of chromogenic (thermotropic and thermochromic) materials in GUs.

Ref.	Chromogenic Material	Climate Code	Study Type	Envelope Element	Application	Findings and Remarks
[90]	NaCl + HPMC + Water	Cfa	N	DGW	Cooling and heating	• 70% and 50% reduction in peak undesired indoor temperature is reported versus conventional DGWs and tinted DGWs, respectively.
[91]	n-alkane mixture	Cfa	E	TGW	Cooling and heating	• PCM and thermotropic layers are used at the same time. It is suggested to place PCM and thermotropic layers in the innermost and outermost cavity spaces, respectively.
[92]	HPC polymer	Cfb	N	DGW	Cooling and heating	• Glazing system reflectance above and below threshold temperature of the thermotropic layer is reported as 70% and 10%, respectively. Authors also used a PV layer in the DGW. • Hydroxypropyl cellulose polymer is a potential thermotropic material for the application of smart windows based on their empirical findings.
[93]	parallel slat	Cfb, Csa, Dfb, Af	E, N	DGW	Cooling and heating	• 27.1% enhancement in annual energy saving is reported by the use of thermotropic material in a DGW compared to a conventional DGW.
[94]	parallel slat	Cfb	N	DGW	Cooling and heating	• 22% enhancement in building energy performance is reported by the use of thermotropic material in a DGW compared to a conventional DGW.

Table 8. *Cont.*

Ref.	Chromogenic Material	Climate Code	Study Type	Envelope Element	Application	Findings and Remarks
[95]	VO_2	Cfa	E	DGW	Cooling and heating	• The synergetic use of PCM and VO_2 materials showed better indoor thermal comfort than sole passive methods in the cooling period.
[96]	VO_2	Cfa	N	DGW, TGW	Cooling and heating	• The proposed system decreases the total heat gain versus the traditional DGWs by up to 32% and 40% for a sunny and cloudy day, respectively, while during winter, the proposed system is not as sufficient as DGW due to the block of desirable solar energy.
[97]	Tetra-fish-inspired layer	Cwa, Aw, Dwa, Af	E	SGW	Cooling and heating	• 35.9 kWh/m^2 enhancement in annual energy saving of an office building is reported for the three studied different climatic conditions.
[98]	Six different thermotropic materials	Cfa	N	DGW	Cooling and heating	• The best performance of thermochromic smart glazing occurs in regions with long summer days and substantially lower solar radiation in winter days.

The last potential passive technology for smart glazing discussed in this article is chromogenic materials. The objective is to evaluate the viability of combining these materials with other passive technologies in order to achieve the desired energy performance in GUs. There are several individual applications of chromogenic materials, but only a few use them in combination with other smart glazing techniques. Using their dynamic control of the sunlight entering buildings, PCM overheating may be prevented, and other technologies can work in a safer environment. They function better in locations with warm summers (climatic code ending in "a").

4. Summary and Conclusions

The transparent parts in the building envelopes are responsible for the most energy losses. The initial sources of these energy losses came from burning fossil fuels. As such, the heat losses from building envelopes also contribute to global warming and CO_2 emissions. Increasing demand for the use of fully glazed façade systems makes it essential to optimize the energy performance of these systems. This study reviewed the potential active and passive methods, focusing on phase change materials (PCMs) as latent energy storage material for energy enhancement of fenestration systems while providing a desirable optical view, as well as enough sunlight for the occupants. Other technologies were also reviewed for smart glazing combined with PCM, including shading systems, solar cells (photovoltaic), and chromogenic (thermotropic and thermochromic). Since the climatic condition has been identified as the most influential factor for choosing the appropriate technology for smart glazing systems, almost all reviewed studies in this paper were designated by a Köppen-Geiger climate classification code. The main observations of this review study are as follows:

- PCM performs better in places where solar heat gain is greater. In addition, PCM is more successful in the summer and on clear days, whereas its efficacy in the winter and on overcast days is uncertain, necessitating the use of other passive and active approaches such as night ventilation.

- The PCM's volume expansion during phase transition is an additional factor that must be considered. Another potential problem that has been discussed is the reduced solar transmittance of PCM solid phase in comparison to liquid phase. Using solid–solid translucent PCM, which can also remove leakage and volume-changing issues, is one way to avoid this problem.
- During the summer, when the PCM-integrated blind system is on the interior side of the GUs, the absorbed daytime heat must not be vented inside, necessitating nighttime ventilation. On the other hand, during winter it collects heat during the daytime and releases it to the inside, which is a beneficial effect, but it filters more sunlight during the day as additional opaque material has been added to the blind system. To minimize losing sunlight, cascaded PCM integration with multiple MTs is recommended.
- Combining a PV layer and a PCM layer in the glazing units appears to be a promising technique that requires additional research to be fully exploited. The PCM enables the PV module to operate safely, which improves the thermal performance of the smart glazing system. As the PV layer blocks sunlight transmittance, it might be employed to keep the PCM from overheating while also producing electricity.
- Since PV-window technology alone has been used more frequently than in combination with other smart glazing technologies, and has demonstrated a promising energy-saving performance, it could be combined with other passive technologies to achieve a higher thermal performance for smart glazing technology. In addition, solar cells show better performance in regions with less cloudy days.
- There are numerous individual utilizations of chromogenic materials, but only a few use them in combination with other passive techniques. Using their dynamic control of the sunlight entering buildings, PCM overheating may be prevented, and other technologies can work in a safer environment. They function better in locations with warm summers.

As per this review study, the scientific gaps for future works would include the following:

- An unsteady state analysis of the use of PCMs, along with other glazing technologies, over a long period of time is missing in the literature, as the available studies were mainly conducted on typical days in summer and winter.
- The hysteresis analysis for a large number of cycles for PCMs, as well as PV and chromogenic layers, is missing in the literature.
- A hygrothermal analysis and risk of mold growth due to using PCM combined with other technologies in the glazing systems is missing in the literature.
- The use of various technologies in smart glazing and identifying the optimum case for each climatic condition is also less studied in the literature.
- Incorporating Prisma glasses with other technologies to enhance the energy performance of the glazing units needs to be expanded to cover various operating conditions.
- The economic viability of incorporating PCMs in smart glazing is not justified in previous studies.
- Optical characteristics of smart glazing are of vital importance and need to be studied more deeply.

Author Contributions: Conceptualization, H.A., W.M. and H.H.S.; methodology, H.A., W.M. and H.H.S.; formal analysis, H.A.; investigation, H.A.; resources, H.A.; Writing—Original draft preparation, H.A.; Writing—Review and editing, H.A., W.M. and H.H.S.; visualization, H.A.; supervision, W.M. and H.H.S.; project administration, W.M. and H.H.S. All authors have read and agreed to the published version of the manuscript.

Funding: This research received no external funding.

Data Availability Statement: Not applicable.

Conflicts of Interest: The authors declare no conflict of interest.

Nomenclature

List of symbols

P_{dry}	Precipitation in the driest month (mm month^{-1})
P_{sdry}	Precipitation in the driest month in summer (mm month^{-1})
P_{wdry}	Precipitation in the driest month in winter (mm month^{-1})
P_{swet}	Precipitation in the wettest month in summer (mm month^{-1})
P_{wwet}	Precipitation in the wettest month in winter (mm month^{-1})
T	Temperature (°C)
T_{cold}	The air temperature of the coldest month (°C)
T_{hot}	The air temperature of the warmest month (°C)
T_{mon10}	The number of months with air temperature >10 °C

Abbreviations

a-Si	Amorphous Silicon
CdTe	Cadmium telluride
CFD	Computational fluid dynamics
DG	Double glazing
DGU	Double glazing unit
DGW	Double glazing window
DSF	Double skin facade
DSSC	Dye-sensitized solar cell
EVA	Ethylene vinyl acetate
GU	Glazing unit
HISG	High insulation solar glass
HPC	Hydroxypropyl cellulose
LCST	Lower critical solution temperature
MAT	Mean annual air temperature (°C)
MAP	Mean annual precipitation (mm y^{-1})
MT	Melting temperature
ND	n-docosane
NE	n-eicosane
NO	n-octadecane
SIS	Switchable insulation systems
TES	Thermal energy storage
TG	Triple glazing
TGU	Triple glazing unit
TGF	Triple glazing façade
TSF	Triple skin façade
PCM	Phase Change Material
PSC	Perovskite solar cell
PV	Photovoltaic
PVB	Photovoltaic-blind
QG	Quadruple-glazing
QGU	Quadruple-glazing unit
WWR	Window-to-wall ratio

References

1. International Energy Agency. Tracking Buildings 2021. Available online: https://www.iea.org/topics/buildings (accessed on 14 January 2023).
2. Zhou, Y.; Zheng, S.; Liu, Z.; Wen, T.; Ding, Z.; Yan, J.; Zhang, G. Passive and active phase change materials integrated building energy systems with advanced machine-learning based climate-adaptive designs, intelligent operations, uncertainty-based analysis and optimisations: A state-of-the-art review. *Renew. Sustain. Energy Rev.* **2020**, *130*, 109889. [CrossRef]
3. Wei, L.; Li, G.; Ruan, S.-T.; Qi, H. Dynamic coupled heat transfer and energy conservation performance of multilayer glazing window filled with phase change material in summer day. *J. Energy Storage* **2022**, *49*, 104183. [CrossRef]
4. Liu, R.; Cui, H. Study of thermal performance of building using glass curtain wall with phase change material (PCM). In Proceedings of the 5th International Conference on Information Engineering for Mechanics and Materials, Huhhot, China, 25–26 July 2015; Atlantis Press: Amsterdam, The Netherlands, 2015; pp. 811–817.

5. Zhang, S.; Ma, Y.; Li, D.; Liu, C.; Yang, R. Thermal performance of a reversible multiple-glazing roof filled with two PCM. *Renew. Energy* **2022**, *182*, 1080–1093. [CrossRef]
6. Sun, X.; Zhang, Y.; Xie, K.; Medina, M.A. A parametric study on the thermal response of a building wall with a phase change material (PCM) layer for passive space cooling. *J. Energy Storage* **2022**, *47*, 103548. [CrossRef]
7. Khattari, Y.; Arid, A.; El Ouali, A.; Kousksou, T.; Janajreh, I. CFD study on the validity of using PCM in a controlled cooling ceiling integrated in a ventilated room. *Dev. Built Environ.* **2022**, *9*, 100066. [CrossRef]
8. Sun, W.; Zhang, Y.; Ling, Z.; Fang, X.; Zhang, Z. Experimental investigation on the thermal performance of double-layer PCM radiant floor system containing two types of inorganic composite PCMs. *Energy Build.* **2020**, *211*, 109806. [CrossRef]
9. Huang, Y.; El Mankibi, M.; Cantin, R.; Coillot, M. Application of fluids and promising materials as advanced inter-pane media in multi-glazing windows for thermal and energy performance improvement: A review. *Energy Build.* **2021**, *253*, 111458. [CrossRef]
10. Li, D.; Yang, R.; Arıcı, M.; Wang, B.; Tunçbilek, E.; Wu, Y.; Liu, C.; Ma, Z.; Ma, Y. Incorporating phase change materials into glazing units for building applications: Current progress and challenges. *Appl. Therm. Eng.* **2022**, *210*, 118374. [CrossRef]
11. Li, D.; Zhuang, B.; Chen, Y.; Li, B.; Landry, V.; Kaboorani, A.; Wu, Z.; Wang, X.A. Incorporation technology of bio-based phase change materials for building envelope: A review. *Energy Build.* **2022**, *260*, 111920. [CrossRef]
12. Rathore, P.K.S.; Gupta, N.K.; Yadav, D.; Shukla, S.K.; Kaul, S. Thermal performance of the building envelope integrated with phase change material for thermal energy storage: An updated review. *Sustain. Cities Soc.* **2022**, *79*, 103690. [CrossRef]
13. Hee, W.J.; Alghoul, M.A.; Bakhtyar, B.; Elayeb, O.; Shameri, M.A.; Alrubaih, M.S.; Sopian, K. The role of window glazing on daylighting and energy saving in buildings. *Renew. Sustain. Energy Rev.* **2015**, *42*, 323–343. [CrossRef]
14. Saber, H.H.; Hajiah, A.E. 3D Numerical Modeling for Assessing the Energy Performance of Single-Zone Buildings with and without Phase Change Materials. In *Proceedings of the Gulf Conference on Sustainable Built Environment*; Springer: Berlin/Heidelberg, Germany, 2020; pp. 419–438.
15. Gloriant, F.; Joulin, A.; Tittelein, P.; Lassue, S. Using heat flux sensors for a contribution to experimental analysis of heat transfers on a triple-glazed supply-air window. *Energy* **2021**, *215*, 119154. [CrossRef]
16. Beck, H.E.; Zimmermann, N.E.; McVicar, T.R.; Vergopolan, N.; Berg, A.; Wood, E.F. Present and future Köppen-Geiger climate classification maps at 1-km resolution. *Sci. Data* **2018**, *5*, 180214. [CrossRef]
17. Leśniak, A.; Górka, M. Evaluation of selected lightweight curtain wall solutions using multi criteria analysis. In *Proceedings of the AIP Conference Proceedings*; AIP Publishing LLC: Melville, NY, USA, 2018; Volume 1978, p. 240003.
18. Yu, F.; Wennersten, R.; Leng, J. A state-of-art review on concepts, criteria, methods and factors for reaching 'thermal-daylighting balance'. *Build. Environ.* **2020**, *186*, 107330. [CrossRef]
19. Kottek, M.; Grieser, J.; Beck, C.; Rudolf, B.; Rubel, F. World map of the Köppen-Geiger climate classification updated. *Meteorol. Z.* **2006**, *15*, 259–263. [CrossRef] [PubMed]
20. Khamlich, I.; Zeng, K.; Flamant, G.; Baeyens, J.; Zou, C.; Li, J.; Yang, X.; He, X.; Liu, Q.; Yang, H. Technical and economic assessment of thermal energy storage in concentrated solar power plants within a spot electricity market. *Renew. Sustain. Energy Rev.* **2021**, *139*, 110583. [CrossRef]
21. Navakrishnan, S.; Vengadesan, E.; Senthil, R.; Dhanalakshmi, S. An experimental study on simultaneous electricity and heat production from solar PV with thermal energy storage. *Energy Convers. Manag.* **2021**, *245*, 114614. [CrossRef]
22. Koşan, M.; Aktaş, M. Experimental investigation of a novel thermal energy storage unit in the heat pump system. *J. Clean. Prod.* **2021**, *311*, 127607. [CrossRef]
23. Heier, J.; Bales, C.; Martin, V. Combining thermal energy storage with buildings—A review. *Renew. Sustain. Energy Rev.* **2015**, *42*, 1305–1325. [CrossRef]
24. Hanchi, N.; Hamza, H.; Lahjomri, J.; Oubarra, A. Thermal behavior in dynamic regime of a multilayer roof provided with two phase change materials in the case of a local conditioned. *Energy Procedia* **2017**, *139*, 92–97. [CrossRef]
25. Farid, M.M.; Khudhair, A.M.; Razack, S.A.K.; Al-Hallaj, S. A review on phase change energy storage: Materials and applications. *Energy Convers. Manag.* **2004**, *45*, 1597–1615. [CrossRef]
26. Faraj, K.; Khaled, M.; Faraj, J.; Hachem, F.; Castelain, C. Phase change material thermal energy storage systems for cooling applications in buildings: A review. *Renew. Sustain. Energy Rev.* **2020**, *119*, 109579. [CrossRef]
27. Akeiber, H.; Nejat, P.; Majid, M.Z.A.; Wahid, M.A.; Jomehzadeh, F.; Zeynali Famileh, I.; Calautit, J.K.; Hughes, B.R.; Zaki, S.A. A review on phase change material (PCM) for sustainable passive cooling in building envelopes. *Renew. Sustain. Energy Rev.* **2016**, *60*, 1470–1497. [CrossRef]
28. Wang, Q.; Wu, R.; Wu, Y.; Zhao, C.Y. Parametric analysis of using PCM walls for heating loads reduction. *Energy Build.* **2018**, *172*, 328–336. [CrossRef]
29. Li, D.; Wu, Y.; Wang, B.; Liu, C.; Arıcı, M. Optical and thermal performance of glazing units containing PCM in buildings: A review. *Constr. Build. Mater.* **2020**, *233*, 117327. [CrossRef]
30. Akram, M.W.; Hasannuzaman, M.; Cuce, E.; Cuce, P.M. Global technological advancement and challenges of glazed window, facade system and vertical greenery-based energy savings in buildings: A comprehensive review. *Energy Built Environ.* **2021**, *4*, 206–226. [CrossRef]
31. Goia, F.; Perino, M.; Serra, V. Improving thermal comfort conditions by means of PCM glazing systems. *Energy Build.* **2013**, *60*, 442–452. [CrossRef]

32. Goia, F.; Perino, M.; Serra, V. Experimental analysis of the energy performance of a full-scale PCM glazing prototype. *Sol. Energy* **2014**, *100*, 217–233. [CrossRef]
33. King, M.F.L.; Rao, P.N.; Sivakumar, A.; Mamidi, V.K.; Richard, S.; Vijayakumar, M.; Arunprasath, K.; Kumar, P.M. Thermal performance of a double-glazed window integrated with a phase change material (PCM). *Mater. Today Proc.* **2022**, *50*, 1516–1521. [CrossRef]
34. Liu, C.; Wu, Y.; Zhu, Y.; Li, D.; Ma, L. Experimental investigation of optical and thermal performance of a PCM-glazed unit for building applications. *Energy Build.* **2018**, *158*, 794–800. [CrossRef]
35. Tafakkori, R.; Fattahi, A. Introducing novel configurations for double-glazed windows with lower energy loss. *Sustain. Energy Technol. Assess.* **2021**, *43*, 100919. [CrossRef]
36. Musiał, M. Experimental and Numerical Analysis of the Energy Efficiency of Transparent Partitions with a Thermal Storage Unit. *J. Ecol. Eng.* **2020**, *21*, nr 6. [CrossRef]
37. Musiał, M.; Lichołai, L. The Impact of a Mobile Shading System and a Phase-Change Heat Store on the Thermal Functioning of a Transparent Building Partition. *Materials* **2021**, *14*, 2512. [CrossRef] [PubMed]
38. Duraković, B.; Mešetović, S. Thermal performances of glazed energy storage systems with various storage materials: An experimental study. *Sustain. Cities Soc.* **2019**, *45*, 422–430. [CrossRef]
39. Khetib, Y.; Alotaibi, A.A.; Alshahri, A.H.; Rawa, M.; Cheraghian, G.; Sharifpur, M. Impact of phase change material on the amount of emission in the double-glazed window frame for different window angles. *J. Energy Storage* **2021**, *44*, 103320. [CrossRef]
40. Gao, Y.; Zheng, Q.; Jonsson, J.C.; Lubner, S.; Curcija, C.; Fernandes, L.; Kaur, S.; Kohler, C. Parametric study of solid-solid translucent phase change materials in building windows. *Appl. Energy* **2021**, *301*, 117467. [CrossRef]
41. Yang, R.; Li, D.; Wei, W.; Wang, F. A Mie optimization model to determine optical properties of PCM based nanofluids for solar thermal applications of glazing window. *Optik* **2020**, *212*, 164664. [CrossRef]
42. Li, S.; Zou, K.; Sun, G.; Zhang, X. Simulation research on the dynamic thermal performance of a novel triple-glazed window filled with PCM. *Sustain. Cities Soc.* **2018**, *40*, 266–273. [CrossRef]
43. Wieprzkowicz, A.; Heim, D. Modelling of thermal processes in a glazing structure with temperature dependent optical properties—An example of PCM-window. *Renew. Energy* **2020**, *160*, 653–662. [CrossRef]
44. Liu, C.; Zhang, G.; Arıcı, M.; Bian, J.; Li, D. Thermal performance of non-ventilated multilayer glazing facades filled with phase change material. *Sol. Energy* **2019**, *177*, 464–470. [CrossRef]
45. Kara, Y.A.; Kurnuç, A. Performance of coupled novel triple glass unit and pcm wall. *Appl. Therm. Eng.* **2012**, *35*, 243–246. [CrossRef]
46. Souayfane, F.; Biwole, P.H.; Fardoun, F. Thermal behavior of a translucent superinsulated latent heat energy storage wall in summertime. *Appl. Energy* **2018**, *217*, 390–408. [CrossRef]
47. Maduru, V.R.; Shaik, S. Laminated glazing for buildings: Energy saving, natural daylighting, and CO_2 emission mitigation prospective. *Environ. Sci. Pollut. Res.* **2022**, *29*, 14299–14315. [CrossRef] [PubMed]
48. Weinlaeder, H.; Koerner, W.; Heidenfelder, M. Monitoring results of an interior sun protection system with integrated latent heat storage. *Energy Build.* **2011**, *43*, 2468–2475. [CrossRef]
49. Wang, Q.; Zhao, C.Y. Parametric investigations of using a PCM curtain for energy efficient buildings. *Energy Build.* **2015**, *94*, 33–42. [CrossRef]
50. Silva, T.; Vicente, R.; Rodrigues, F.; Samagaio, A.; Cardoso, C. Development of a window shutter with phase change materials: Full scale outdoor experimental approach. *Energy Build.* **2015**, *88*, 110–121. [CrossRef]
51. Silva, T.; Vicente, R.; Rodrigues, F.; Samagaio, A.; Cardoso, C. Performance of a window shutter with phase change material under summer Mediterranean climate conditions. *Appl. Therm. Eng.* **2015**, *84*, 246–256. [CrossRef]
52. Silva, T.; Vicente, R.; Amaral, C.; Figueiredo, A. Thermal performance of a window shutter containing PCM: Numerical validation and experimental analysis. *Appl. Energy* **2016**, *179*, 64–84. [CrossRef]
53. Park, J.H.; Yun, B.Y.; Chang, S.J.; Wi, S.; Jeon, J.; Kim, S. Impact of a passive retrofit shading system on educational building to improve thermal comfort and energy consumption. *Energy Build.* **2020**, *216*, 109930. [CrossRef]
54. Li, Y.; Darkwa, J.; Kokogiannakis, G.; Su, W. Phase change material blind system for double skin façade integration: System development and thermal performance evaluation. *Appl. Energy* **2019**, *252*, 113376. [CrossRef]
55. Hu, Y.; Guo, R.; Heiselberg, P.K. Performance and control strategy development of a PCM enhanced ventilated window system by a combined experimental and numerical study. *Renew. Energy* **2020**, *155*, 134–152. [CrossRef]
56. Elarga, H.; Goia, F.; Zarrella, A.; Dal Monte, A.; Benini, E. Thermal and electrical performance of an integrated PV-PCM system in double skin façades: A numerical study. *Sol. Energy* **2016**, *136*, 112–124. [CrossRef]
57. Elarga, H.; Dal Monte, A.; Andersen, R.K.; Benini, E. PV-PCM integration in glazed building. Co-simulation and genetic optimization study. *Build. Environ.* **2017**, *126*, 161–175. [CrossRef]
58. Ziasistani, N.; Fazelpour, F. Comparative study of DSF, PV-DSF and PV-DSF/PCM building energy performance considering multiple parameters. *Sol. Energy* **2019**, *187*, 115–128. [CrossRef]
59. Heydari, A.H.; Haghighi Khoshkhoo, R. Techno-economical analysis of DSF, BIPV and PCM in administrative buildings in four climates of Iran. *Int. J. Ambient Energy* **2022**, *43*, 8474–8485. [CrossRef]
60. Ahmed, M.; Radwan, A.; Serageldin, A.; Memon, S.; Katsura, T.; Nagano, K. Thermal Analysis of a New Sliding Smart Window Integrated with Vacuum Insulation, Photovoltaic, and Phase Change Material. *Sustainability* **2020**, *12*, 7846. [CrossRef]

61. Ke, W.; Ji, J.; Wang, C.; Zhang, C.; Xie, H.; Tang, Y.; Lin, Y. Comparative analysis on the electrical and thermal performance of two CdTe multi-layer ventilated windows with and without a middle PCM layer: A preliminary numerical study. *Renew. Energy* **2022**, *189*, 1306–1323. [CrossRef]
62. Cuce, E.; Cuce, P.M.; Young, C.-H. Energy saving potential of heat insulation solar glass: Key results from laboratory and in-situ testing. *Energy* **2016**, *97*, 369–380. [CrossRef]
63. Sharma, M.K.; Preet, S.; Mathur, J.; Chowdhury, A.; Mathur, S. Exploring the advantages of photo-voltaic triple skin façade in hot summer conditions. *Sol. Energy* **2021**, *217*, 317–327. [CrossRef]
64. Tang, Y.; Ji, J.; Wang, C.; Xie, H.; Ke, W. Performance prediction of a novel double-glazing PV curtain wall system combined with an air handling unit using exhaust cooling and heat recovery technology. *Energy Convers. Manag.* **2022**, *265*, 115774. [CrossRef]
65. Luo, Y.; Zhang, L.; Wang, X.; Xie, L.; Liu, Z.; Wu, J.; Zhang, Y.; He, X. A comparative study on thermal performance evaluation of a new double skin façade system integrated with photovoltaic blinds. *Appl. Energy* **2017**, *199*, 281–293. [CrossRef]
66. Tan, Y.; Peng, J.; Luo, Y.; Luo, Z.; Curcija, C.; Fang, Y. Numerical heat transfer modeling and climate adaptation analysis of vacuum-photovoltaic glazing. *Appl. Energy* **2022**, *312*, 118747. [CrossRef]
67. Uddin, M.M.; Wang, C.; Zhang, C.; Ji, J. Investigating the energy-saving performance of a CdTe-based semi-transparent photovoltaic combined hybrid vacuum glazing window system. *Energy* **2022**, *253*, 124019. [CrossRef]
68. Wang, C.; Uddin, M.M.; Ji, J.; Yu, B.; Wang, J. The performance analysis of a double-skin ventilated window integrated with CdTe cells in typical climate regions. *Energy Build.* **2021**, *241*, 110922. [CrossRef]
69. Alrashidi, H.; Issa, W.; Sellami, N.; Sundaram, S.; Mallick, T. Thermal performance evaluation and energy saving potential of semi-transparent CdTe in Façade BIPV. *Sol. Energy* **2022**, *232*, 84–91. [CrossRef]
70. Zhang, C.; Ji, J.; Wang, C.; Ke, W.; Xie, H.; Yu, B. Experimental and numerical studies on the thermal and electrical performance of a CdTe ventilated window integrated with vacuum glazing. *Energy* **2022**, *244*, 123128. [CrossRef]
71. Castillo, M.S.; Liu, X.; Abd-AlHamid, F.; Connelly, K.; Wu, Y. Intelligent windows for electricity generation: A technologies review. In *Proceedings of the Building Simulation*; Springer: Berlin/Heidelberg, Germany, 2022; pp. 1–27.
72. Musameh, H.; Alrashidi, H.; Al-Neami, F.; Issa, W. Energy performance analytical review of semi-transparent photovoltaics glazing in the United Kingdom. *J. Build. Eng.* **2022**, *54*, 104686. [CrossRef]
73. Yu, G.; Yang, H.; Luo, D.; Cheng, X.; Ansah, M.K. A review on developments and researches of building integrated photovoltaic (BIPV) windows and shading blinds. *Renew. Sustain. Energy Rev.* **2021**, *149*, 111355. [CrossRef]
74. Wang, C.; Ji, J.; Uddin, M.M.; Yu, B.; Song, Z. The study of a double-skin ventilated window integrated with CdTe cells in a rural building. *Energy* **2021**, *215*, 119043. [CrossRef]
75. Qiu, C.; Yang, H. Dynamic coupling of a heat transfer model and whole building simulation for a novel cadmium telluride-based vacuum photovoltaic glazing. *Energy* **2022**, *250*, 123745. [CrossRef]
76. Wang, C.; Li, N.; Yu, B.; Uddin, M.M.; Ji, J. A novel solar spectrum-splitting utilization photocatalytic CdTe double-skin façade: Concept, design and performance investigation. *Build. Environ.* **2021**, *195*, 107776. [CrossRef]
77. Su, X.; Zhang, L.; Luo, Y.; Liu, Z.; Yang, H.; Wang, X. Conceptualization and preliminary analysis of a novel reversible photovoltaic window. *Energy Convers. Manag.* **2021**, *250*, 114925. [CrossRef]
78. Wang, C.; Ji, J.; Yu, B.; Zhang, C.; Ke, W.; Wang, J. Comprehensive investigation on the luminous and energy-saving performance of the double-skin ventilated window integrated with CdTe cells. *Energy* **2022**, *238*, 121757. [CrossRef]
79. Su, X.; Zhang, L.; Luo, Y.; Liu, Z. Energy performance of a reversible window integrated with photovoltaic blinds in Harbin. *Build. Environ.* **2022**, *213*, 108861. [CrossRef]
80. Touma, A.A.; Ouahrani, D. Shading and day-lighting controls energy savings in offices with fully-Glazed façades in hot climates. *Energy Build.* **2017**, *151*, 263–274. [CrossRef]
81. Dutta, A.; Samanta, A.; Neogi, S. Influence of orientation and the impact of external window shading on building thermal performance in tropical climate. *Energy Build.* **2017**, *139*, 680–689. [CrossRef]
82. Fedorczak-Cisak, M.; Nowak, K.; Furtak, M. Analysis of the effect of using external venetian blinds on the thermal comfort of users of highly glazed office rooms in a transition season of temperate climate—Case study. *Energies* **2019**, *13*, 81. [CrossRef]
83. Kuczyński, T.; Staszczuk, A.; Gortych, M.; Stryjski, R. Effect of thermal mass, night ventilation and window shading on summer thermal comfort of buildings in a temperate climate. *Build. Environ.* **2021**, *204*, 108126. [CrossRef]
84. Carlier, R.; Dabbagh, M.; Krarti, M. Energy Performance of Integrated Wall and Window Switchable Insulated Systems for Residential Buildings. *Energies* **2022**, *15*, 1056. [CrossRef]
85. Wang, Z.; Tian, Q.; Jia, J. Numerical study on performance optimization of an energy-saving insulated window. *Sustainability* **2021**, *13*, 935. [CrossRef]
86. Cho, H.M.; Yang, S.; Wi, S.; Chang, S.J.; Kim, S. Hygrothermal and energy retrofit planning of masonry façade historic building used as museum and office: A cultural properties case study. *Energy* **2020**, *201*, 117607. [CrossRef]
87. Tan, Y.; Peng, J.; Luo, Y.; Gao, J.; Luo, Z.; Wang, M.; Curcija, D.C. Parametric study of venetian blinds for energy performance evaluation and classification in residential buildings. *Energy* **2022**, *239*, 122266. [CrossRef]
88. Zhang, C.; Gang, W.; Wang, J.; Xu, X.; Du, Q. Experimental investigation and dynamic modeling of a triple-glazed exhaust air window with built-in venetian blinds in the cooling season. *Appl. Therm. Eng.* **2018**, *140*, 73–85. [CrossRef]
89. Seeboth, A.; Ruhmann, R.; Mühling, O. Thermotropic and thermochromic polymer based materials for adaptive solar control. *Materials* **2010**, *3*, 5143–5168. [CrossRef]

90. Yao, J.; Zhu, N. Evaluation of indoor thermal environmental, energy and daylighting performance of thermotropic windows. *Build. Environ.* **2012**, *49*, 283–290. [CrossRef]
91. Goia, F.; Bianco, L.; Cascone, Y.; Perino, M.; Serra, V. Experimental analysis of an advanced dynamic glazing prototype integrating PCM and thermotropic layers. *Energy Procedia* **2014**, *48*, 1272–1281. [CrossRef]
92. Connelly, K.; Wu, Y.; Ma, X.; Lei, Y. Transmittance and reflectance studies of thermotropic material for a novel building integrated concentrating photovoltaic (BICPV)'smart window'system. *Energies* **2017**, *10*, 1889. [CrossRef]
93. Sun, Y.; Liu, X.; Ming, Y.; Liu, X.; Mahon, D.; Wilson, R.; Liu, H.; Eames, P.; Wu, Y. Energy and daylight performance of a smart window: Window integrated with thermotropic parallel slat-transparent insulation material. *Appl. Energy* **2021**, *293*, 116826. [CrossRef]
94. Sun, Y.; Wilson, R.; Liu, H.; Wu, Y. Numerical investigation of a smart window system with thermotropic Parallel Slat Transparent Insulation Material for building energy conservation and daylight autonomy. *Build. Environ.* **2021**, *203*, 108048. [CrossRef]
95. Long, L.; Ye, H.; Gao, Y.; Zou, R. Performance demonstration and evaluation of the synergetic application of vanadium dioxide glazing and phase change material in passive buildings. *Appl. Energy* **2014**, *136*, 89–97. [CrossRef]
96. Jin, Q.; Long, X.; Liang, R. Numerical analysis on the thermal performance of PCM-integrated thermochromic glazing systems. *Energy Build.* **2022**, *257*, 111734. [CrossRef]
97. Ke, Y.; Tan, Y.; Feng, C.; Chen, C.; Lu, Q.; Xu, Q.; Wang, T.; Liu, H.; Liu, X.; Peng, J.; et al. Tetra-Fish-Inspired aesthetic thermochromic windows toward Energy-Saving buildings. *Appl. Energy* **2022**, *315*, 119053. [CrossRef]
98. Tao, Y.; Fang, X.; Zhang, H.; Zhang, G.; Tu, J.; Shi, L. Impacts of thermo-optical properties on the seasonal operation of thermochromic smart window. *Energy Convers. Manag.* **2022**, *252*, 115058. [CrossRef]
99. Lin, K.; Chao, L.; Lee, H.H.; Xin, R.; Liu, S.; Ho, T.C.; Huang, B.; Yu, K.M.; Tso, C.Y. Potential building energy savings by passive strategies combining daytime radiative coolers and thermochromic smart windows. *Case Stud. Therm. Eng.* **2021**, *28*, 101517. [CrossRef]
100. Arnesano, M.; Pandarese, G.; Martarelli, M.; Naspi, F.; Gurunatha, K.L.; Sol, C.; Portnoi, M.; Ramirez, F.V.; Parkin, I.P.; Papakonstantinou, I.; et al. Optimization of the thermochromic glazing design for curtain wall buildings based on experimental measurements and dynamic simulation. *Sol. Energy* **2021**, *216*, 14–25. [CrossRef]
101. Arnaoutakis, G.E.; Katsaprakakis, D.A. Energy Performance of Buildings with Thermochromic Windows in Mediterranean Climates. *Energies* **2021**, *14*, 6977. [CrossRef]
102. Hong, X.; Shi, F.; Wang, S.; Yang, X.; Yang, Y. Multi-objective optimization of thermochromic glazing based on daylight and energy performance evaluation. In *Proceedings of the Building Simulation*; Springer: Berlin/Heidelberg, Germany, 2021; Volume 14, pp. 1685–1695.
103. Teixeira, H.; Glória Gomes, M.; Moret Rodrigues, A.; Aelenei, D. Assessment of the visual, thermal and energy performance of static vs. thermochromic double-glazing under different European climates. *Build. Environ.* **2022**, *217*, 109115. [CrossRef]
104. Wang, S.; Zhou, Y.; Jiang, T.; Yang, R.; Tan, G.; Long, Y. Thermochromic smart windows with highly regulated radiative cooling and solar transmission. *Nano Energy* **2021**, *89*, 106440. [CrossRef]
105. Aburas, M.; Ebendorff-Heidepriem, H.; Lei, L.; Li, M.; Zhao, J.; Williamson, T.; Wu, Y.; Soebarto, V. Smart windows—Transmittance tuned thermochromic coatings for dynamic control of building performance. *Energy Build.* **2021**, *235*, 110717. [CrossRef]